

# *Stratigraphic evolution of intraslope minibasins: Insights from surface-based model*

**Zoltán Sylvester, Alessandro Cantelli, and Carlos Pirmez**

## **ABSTRACT**

Although numerous case studies exist to illustrate the large-scale stratigraphic architecture of salt-withdrawal minibasins, there is no clear understanding of how stratal patterns emerge as a function of the interplay between basin subsidence and sedimentation. Here we present a simple model of mass balance in minibasin sedimentation that focuses on the interaction between long-term sediment supply and basin-wide subsidence rate. The model calculates the sediment flux in three dimensions assuming a simplified basin and deposit geometry. The main model output is a cross section that captures the large-scale stratigraphic patterns. This architecture is determined by the relative movement of the stratal terminations along the basin margin: consecutive pinchout points can (1) be stationary, (2) move toward the basin edge (onlap), or (3) move toward the basin center (offlap). The direction and magnitude of this movement depend on the balance between the volume made available through subsidence, calculated only over the area of the previous deposit, and the volume needed to accommodate all the sediment that comes into the basin. Cycles of increasing-to-decreasing sediment supply result in stratigraphic sequences with an onlapping lower part and offlapping upper part. If the sediment input curve is more similar to a step function, stratigraphic sequences only consist of an onlapping sediment package, with no offlap at the top. Modeling two linked basins in which deposition takes place during ongoing subsidence shows that conventional static fill-and-spill models cannot correctly capture the age relationships between basin fills. In general, lower sediment input rates and periods of sediment bypass result in sand-poor convergent stratal patterns, and episodic but high volumetric sedimentation rates lead to well-defined onlap with an increased probability of high sand content.

---

Copyright ©2015. The American Association of Petroleum Geologists. All rights reserved.

Manuscript received May 12, 2014; provisional acceptance September 18, 2014; revised manuscript received November 26, 2014; final acceptance January 8, 2015.

DOI: 10.1306/01081514082

## **AUTHORS**

**ZOLTÁN SYLVESTER** ~ *Shell Research and Development, Houston, Texas; present address: Chevron Energy Technology Company, Houston, Texas;*  
*zoltan.sylvester@gmail.com*

Zoltán Sylvester holds degrees in geology from Babeş-Bolyai University (Romania) and Stanford University. After more than 10 years of work on deep-water reservoirs at Shell's Research Center in Houston, in 2014, he joined the Clastic Stratigraphy R&D group at Chevron where his interests continue to cover a wide range of scales, from sand grains to seismic volumes.

**ALESSANDRO CANTELLI** ~ *Shell Exploration and Production, Houston, Texas;*  
*alessandro.cantelli@shell.com*

Alessandro Cantelli has a Ph.D. in fluid mechanics from the University of Genoa. After focusing on experimental studies as a research associate at the University of Minnesota and University of Illinois, he joined Shell R&D in 2006. He works at the edges between geology and physics, developing and applying numerical and physical models to better understand sedimentary systems.

**CARLOS PIRMEZ** ~ *Shell Italia E&P, Rome, Italy;*  
*carlos.pirmez@shell.com*

Carlos Pirmez received a B.S. degree in oceanography from the Universidade do Estado do Rio de Janeiro and a Ph.D. in marine geology and geophysics from Columbia University. He has worked on the sedimentary geology of deep-water depositional systems in outcrops, modern seafloor, flume tanks, and numerical models, with applications to the exploration and development of turbidite reservoirs. He now works at Shell Italia E&P on the production geology and development of fractured carbonate reservoirs.

## **ACKNOWLEDGEMENTS**

We are thankful for discussions on various aspects of minibasin stratigraphy and modeling with Brad Prather, Charles Winker, Gary Steffens, Nick Howes, Matt Wolinsky,

and Zane Jobe; and for comments and suggestions by journal reviewers Andrew Madof and Steve Hubbard. We also thank Shell International Exploration and Production Inc. for support to conduct and publish this work.

## DATASHARE 63

Movies 1–10 are available on the AAPG website ([www.aapg.org/datashare](http://www.aapg.org/datashare)) as Datashare 63.

## EDITOR'S NOTE

Color versions of Figures 1, 13–14, and 16 can be seen in the online version of this paper.

## INTRODUCTION

Several continental margins in the world are strongly affected by plastic deformation of deeply buried, thick salt accumulations that were deposited during early basin evolution (Hudec and Jackson, 2007). A wide range of salt morphologies result from differential loading of salt by overlying sediments, and patterns of sedimentation are also strongly influenced by the deformation of underlying evaporites (e.g., Prather et al., 1998; Hudec and Jackson, 2007; Pilcher et al., 2011; Peel, 2014). One of the most common expressions of this salt-sediment interaction are salt-withdrawal minibasins (Figure 1), quasicircular or oval depressions on continental slopes that can capture a large proportion of the sediment, which is transported from shallow to deep waters by turbidity currents and other sediment gravity flows (Pratson and Ryan, 1994; Steffens et al., 2003). Because sand can be preferentially trapped in these depressions, intraslope basins are common sites of thick, sand-rich accumulations, and ancient, buried basins host significant hydrocarbon reservoirs (Mahaffie, 1994; Prather et al., 1998; Kendrick, 2000; Booth et al., 2003). Intraslope basins with ponded accommodation (*sensu* Steffens et al., 2003) can also form on continental margins without salt tectonics. For example, the California Continental Borderland is dominated by strike-slip deformation and shows several deep basins separated by high sills (Teng and Gorsline, 2008). Sedimentary processes in these basins are comparable to those operating in salt-related slope basins in the Gulf of Mexico (Covault and Romans, 2009).

Over the last two decades, significant progress has been made in the understanding of (1) the large-scale stratigraphic architecture and evolution of salt-withdrawal minibasins (Mahaffie, 1994; Pratson and Ryan, 1994; Winker, 1996; Prather et al., 1998; Badalini et al., 2000; Beaubouef and Friedmann, 2000; Booth et al., 2000; Winker and Booth, 2000; Meckel et al., 2002; Sinclair and Tomasso, 2002; Booth et al., 2003; Smith, 2004; Beaubouef and Abreu, 2006; Mallarino et al., 2006; Madof et al., 2009; Pirmez et al., 2012; Prather et al., 2012a, b) and (2) the behavior of turbidity currents entering the basins and the resulting fine-scale depositional features (Brunt et al., 2004; Lamb et al., 2004, 2006; Smith and Joseph, 2004; Toniolo et al., 2006a, b; Khan and Imran, 2008; Viparelli et al., 2012). However, these studies have largely focused on sedimentary processes, and the effects of basin subsidence on the stratigraphic architecture have received limited attention. Although synkinematic and episodic sedimentation has been the focus of significant research on the formation of near-salt folds, unconformities, and halokinetic sequences during passive diapirism (Giles and Lawton, 2002; Rowan et al., 2003; Schultz-Ela, 2003;

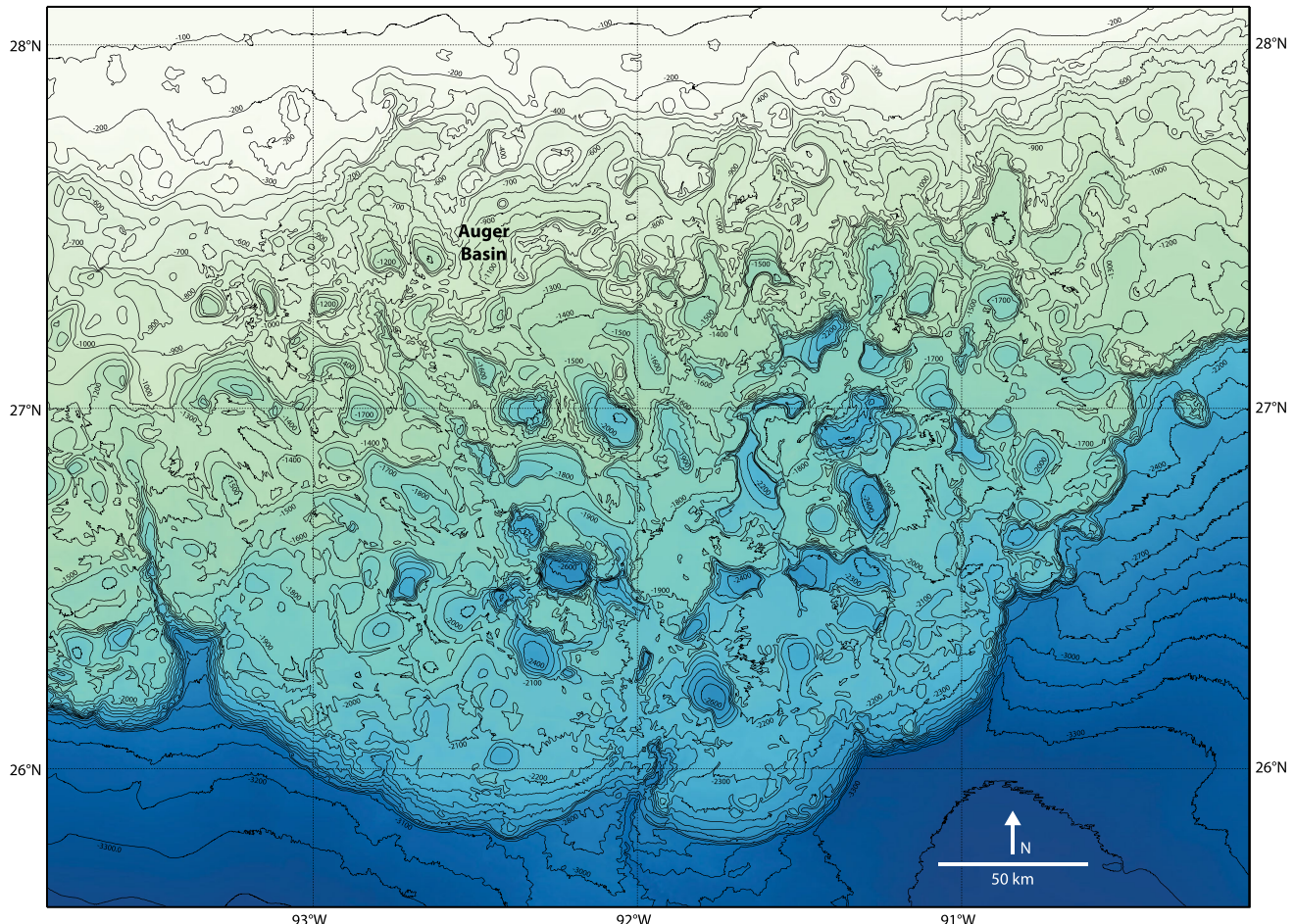


**Figure 1.** Bathymetric map of the central part of the Gulf of Mexico continental slope. Data from the global multi-resolution topography synthesis (Ryan et al., 2009).

Giles and Rowan, 2012), this line of work has not addressed the origin of larger-scale stratigraphic patterns, either.

The origin of large-scale stratal patterns has been discussed extensively within the framework of conventional sequence stratigraphic analysis, with an emphasis on how changes in sea level and sediment supply affect the stratigraphic architecture of shelf-edge settings and result in a variety of clinoform geometries and stratal termination patterns (e.g., Vail et al., 1977; Jervey, 1988; Posamentier et al., 1988; Helland-Hansen and Hampson, 2009). In contrast, the stratigraphy of deep-water minibasins is only indirectly affected by sea-level changes, and clinoforms are essentially absent. The exact meaning of accommodation in shelf-edge settings is the subject of debate (Muto and Steel, 2000); yet it has a clear significance in the case of a minibasin: it is the

unfilled basin volume that lies below the basin spill-point (the ponded accommodation of Steffens et al., 2003). In general, the formation of stratigraphic sequences (or unconformity-bounded packages) in minibasins is a simpler process than the development of sequence boundaries in coastal and shelf-margin settings; yet this process and the resulting stratigraphic patterns have not been the subject of quantitative analysis.

Typical intraslope basins are large enough that only relatively small parts can be seen even in large outcrops (Smith and Joseph, 2004; Bakke et al., 2013). The importance of these basins on certain continental slopes has only been recognized after seismic reflection profiles have become widely available. Prather et al. (1998) described several seismic facies characteristic of slope minibasin fills: in terms of large-scale stratigraphic architecture, the two most

important ones are the convergent baselapping ( $C_b$ ) and convergent thinning ( $C_t$ ) facies. These can be distinguished based on the presence ( $C_b$ ) or absence ( $C_t$ ) of well-defined onlaps. Prather et al. (1998) have also shown that  $C_b$  facies tend to be more sand rich than seismic units with  $C_t$  geometries.

However, the origin of these different reflection geometries is not addressed in detail by Prather et al. (1998). One possible explanation is variable flow behavior that depends on the dominant grain size of the turbidity current. In this interpretation, mud-rich layers with convergent geometry form high up on basin flanks because of (1) the presence of mud at higher elevations in the flow (flow stratification) and (2) the larger run-up heights of mud-rich turbidity currents (Smith and Joseph, 2004; Bakke et al., 2013). Sand-rich flows have more limited run-up heights and, in combination with steeper basin-margin slopes, result in well-defined onlap at the outcrop scale; this is possibly equivalent to the  $C_b$  facies of Prather et al. (1998) (see Smith and Joseph, 2004). However, the convergence and onlap observed in seismic data of typical resolution are commonly of a significantly larger scale than the geometries observed in outcrops, and it is likely that at this scale long-term sedimentation and subsidence rates are more important than flow stratification and run-up behavior.

In the present paper, we aim to explore in more detail how subsidence and sediment input interact in minibasins to form unconformity-bounded stratal packages of variable convergence. First, we describe the stratigraphic forward model and illustrate model results for scenarios of increasing complexity: from end-member convergence and onlap to set-ups with varying sediment input and bypass. Then, we use the model to reproduce the large-scale stratigraphic patterns in two intraslope basins from the Gulf of Mexico.

## MODEL DESCRIPTION

We have developed a simple model that captures the large-scale features of minibasin subsidence and sedimentation. We ignore the details of grain-size fractionation taking place during deposition from a single flow, fractionation that can take place either from the proximal to the distal part of one basin (e.g., Paola and Martin, 2012), or between two basins

(Brunt et al., 2004). Instead, we focus on the overall mass balance of the system, driven by the interplay between sediment supply and subsidence. We do this using a rigid-lid model, with mass balance and variations in sediment supply added (Paola, 2000).

To model basin shape and subsidence, we consider a circular plan-view shape for the basin and either a Gaussian or a parabolic subsidence pattern, with zero subsidence at the basin edge and a maximum value in the middle. The subsidence rate  $S(x, y)$  varies spatially, along both the  $x$  and  $y$  dimensions. An important variable is the volumetric subsidence rate  $\eta$ , which is the volume added to the basin over a unit of time. We do not address here the driving forces and the relationships between sediment loading and salt deformation. The model is applied at a large temporal scale, with time steps significantly longer (tens to thousands of years) than the duration of individual sediment gravity flows (a few days at maximum). In each time step of the model, multiple flows can occur, but flows are not modeled individually; instead, their sediment volume is averaged into a volumetric sediment discharge,  $Q_{in}$ . The length of the time step has to be small enough to capture well the variation in sediment supply but large enough so that averaging over some flows is justified. Because  $Q_{in}$  and  $\eta$  have the same units (volume/time), they can be compared to each other.

At this scale, we can ignore depositional topography, that is, the non-zero dip of depositional surfaces in the basin fill. These dips are commonly less than approximately  $1^\circ$  and impossible to reconstruct from typical seismic images of ancient minibasins. Thus, all sediment from turbidity currents is assumed to be deposited at the bottom of the basin, with a horizontal depositional surface at the top. Data from basins visible on the modern-day seafloor suggest that this is a reasonable assumption (Pratson and Ryan, 1994; Steffens et al., 2003; Pirmez et al., 2012). At each time step, the deposit volume between this surface and the preexisting topography of the basin matches the input sediment volume, with the pore space added

$$V_{dep}(i) = Q_{in}(i)(1 + \varphi)\Delta t \quad (1)$$

where  $V_{dep}(i)$  is the deposit volume at time step  $i$ ,  $\Delta t$  is the length of the time step (total time of simulation

divided by the number of time steps),  $Q_{\text{in}}(i)$  is the volumetric sediment discharge at time step  $i$ , and  $\varphi$  is the average porosity.

In the next time step, the new depositional surface is deformed by subsidence and becomes part of the new basin configuration. A line of onlap will form where the new surface intersects the preexisting basin topography (Figure 2A).

Although channelization and erosion can be significant both near the entry and exit points of the basin, at the scale modeled here minibasins are overall depositional in nature, and we do not include erosional processes. We also ignore compaction; compaction will affect the subsidence pattern to some degree but the effect is deemed of second order and could be added later to the model.

If the incoming sediment volume exceeds the available accommodation in a time step, that is, the unfilled volume of the basin  $V_{\text{acc}}$ , the extra sediment

is transferred to the next basin downdip, and the sediment discharge feeding the next basin will be

$$Q_{\text{out}}(i) = Q_{\text{in}}(i) - V_{\text{acc}}(i)/((1 + \varphi)\Delta t) \quad (2)$$

This modification allows us to investigate sediment partitioning between some basins as a function of their sediment input and subsidence history.

Finally, although this simple model does not include the differential behavior of sand and mud, we attempt to account for pelagic and hemipelagic sedimentation in the form of a mud drape with a spatially and temporally constant sedimentation rate. Unless its thickness is set to zero, this layer is modeled in every time step and it can form a drape of significant thickness if sediment gravity flow supply is limited or nonexistent. These thicker drapes in the model correspond to condensed sections in actual minibasins.

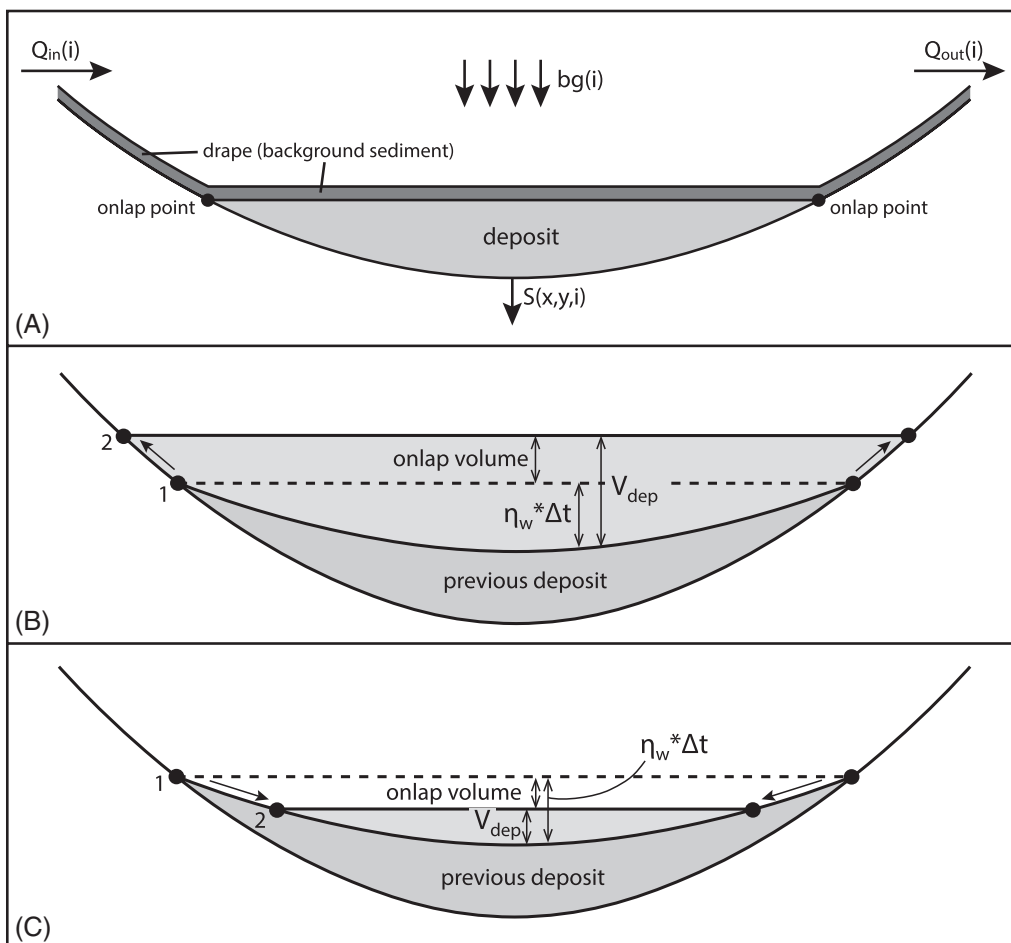


**Figure 2.** (A) Definition sketch of simple model for minibasin filling. See Table 1 for a list of abbreviations. (B) The relative movement of the stratal termination points depends on the balance between the volume needed to accommodate the incoming sediment and the space made available through subsidence on top of previous deposit. When  $V_{\text{dep}} > \eta_w \Delta t$ , the termination points move outward, forming an onlapping stratal pattern. (C) When  $V_{\text{dep}} < \eta_w \Delta t$ , the termination points move toward the basin center and the long-term result is offlap.

**Table 1.** List of Abbreviations

$\eta$	Volumetric subsidence rate ( $\text{m}^3/\text{yr}$ )
$\eta_w$	Volumetric subsidence rate calculated over area of previous deposit ( $\text{m}^3/\text{yr}$ )
$S$	Local subsidence rate ( $\text{m}/\text{yr}$ )
$Q_{\text{in}}$	Volumetric sediment discharge entering the basin ( $\text{m}^3/\text{yr}$ )
$Q_{\text{out}}$	Volumetric sediment discharge leaving the basin ( $\text{m}^3/\text{yr}$ )
$bg$	Background sedimentation rate ( $\text{m}/\text{yr}$ )
$V_{\text{dep}}$	Deposit volume ( $\text{m}^3$ )
$V_{\text{ol}}$	Onlap volume ( $\text{m}^3$ )
$V_{\text{acc}}$	Accommodation ( $\text{m}^3$ )
$V_{\text{bp}}$	Bypass volume ( $\text{m}^3$ )
$\varphi$	Average porosity
OI	Onlap index

To summarize, the model has the following inputs: input sediment discharge  $Q_{\text{in}}$ , subsidence rate  $S(x, y, i)$ , and background sedimentation rate  $bg$ ; and the following outputs: outgoing sediment discharge  $Q_{\text{out}}$ , locations of onlap points, and accommodation  $V_{\text{acc}}$  (Figure 2A).

Realistic rates of sediment input and subsidence were estimated from the well-known case studies in the Gulf of Mexico (see modeling cases 10 and 11). In general, both subsidence and sedimentation rates tend to be high in salt-withdrawal minibasins, with short-term subsidence rates reaching values of 10 km/m.y. (0.01 m/y) in places (Hudec et al., 2008). The values we used in the models shown here are smaller than this (0.001–0.003 m/y) but larger than the spectrum of subsidence rates characteristic of sedimentary basins in general (e.g., Allen and Allen, 2005). To perform the computations and generate the figures, we have used IPython Notebook, an interactive, open access scientific computing platform (Pérez and Granger, 2007).

## RESULTS

In this section, we describe the stratal patterns that result from filling a single basin or two coupled basins, using constant subsidence and different sediment input curves. In each time step, the incoming

sediment volume is placed in the basin and the resulting surface is deformed by the subsidence increment that takes place during the time step (Figure 2A). At the end of the simulation, all the surfaces are plotted in a cross section running through the middle of the basin. In each time step, onlap points are plotted where the new surface terminates against the underlying basin topography. Table 2 shows the input parameters that were used for the 11 cases described later. Movies that illustrate the evolution of stratigraphy through time for certain cases are provided as supplementary material available as AAPG Datashare 63 at [www.aapg.org/datashare](http://www.aapg.org/datashare).

## What Controls the Onlap Curve?

The large-scale stratigraphic architecture in a minibasin is driven by the location of the stratal termination (or pinchout) points through time. One of the key insights of our modeling work is the realization that the trajectory of the termination points is driven by a simple relationship between subsidence and sediment input. Whether these points remain stationary, move toward the basin edges, or move toward the basin center, is determined by the balance between the volume made available through subsidence, calculated only over the area of the previous deposit ( $\eta_w \Delta t$ ), and the volume needed to accommodate all the sediment ( $V_{\text{dep}}$ , Figure 2B, C). If  $V_{\text{dep}} > \eta_w \Delta t$ , additional space is needed to accommodate all the sediment, the pinchout points move toward the edge of the basin, and the lateral extent or width of the new deposit is larger than that of the previous deposit (Figure 2B). If the deposit volume is smaller than what has been made available through subsidence of the previous depositional surface, that is  $V_{\text{dep}} < \eta_w \Delta t$ , the pinchout points move toward the basin center (Figure 2C).

### Case 1: Constant Sediment Input, Shallow Basin: Convergence

First, we investigate the effect of initial basin topography on the stratigraphic architecture. We set the sediment supply to a constant value and the initial basin topography is assumed to be relatively shallow. Because the spatial subsidence pattern and the subsidence rate are constant, the space occupied by the

**Table 2.** Input Parameters Used in the 11 Model Cases

Case Number	1	2	3	4	5	6	7	8	9	10	11
Basin width (km)	10	10	10	10	10	10	10	10	10	15	25
Porosity	0.3	0.3	0.3	0.3	0.3	0.3	0.3	0.3	0.3	0.3	0.3
Total time (1000 yr)	500	500	500	500	500	500	500	500	500	150	2400
Number of time steps	20	10	50	50	25	50	50	50	50	100	200
Sediment input cycles	1	1	3	3	1	3	3	3	3	2	10
Background sed. rate (m/yr)	0	0	0	0	0	0	0	0.00015	0.00015	0.0001	0
Max. sed. input rate ( $m^3/yr$ )	15,000	20,000	30,000	60,000	19,000	30,000	30,000	90,000	90,000	100,000	460,000
Max. subsidence rate (m/yr)	0.0015	0.0015	0.0015	0.0015	0.003	0.003	0.003	0	0.0015	0.002	0.002887
Subsidence curve	Constant	Constant	Constant	Constant	Sinusoidal	Constant	Constant	Step	Step	Step	Decreasing Sinusoidal
Sediment input curve	Constant	Constant	Sinusoidal	Sinusoidal	Shallow	Shallow	Shallow	Deep	Shallow	Shallow	Shallow
Initial basin configuration	Shallow	Deep	5	6	7	8	9	10	11, 12	14, 15	16, 17
Figure number	3	4									

incoming sediment is recreated in each time step through subsidence and the locations of the onlap points do not change (Figure 3). This equilibrium between sediment supply and subsidence results in a perfect convergence of stratigraphic surfaces.

## Case 2: Constant Sediment Input, Deep Basin: Onlap

In a second scenario, we start out with the same sediment supply and subsidence pattern, but the basin already has a significant depth when the sediment starts entering the basin. In this case, the onlap points progressively step toward the basin margin, increasing the area occupied by the new deposit (Figure 4). If everything is kept constant, as the basin fills and the basin area increases, the additional area that is needed to accommodate the incoming sediment becomes smaller through time and the onlap points get closer to each other.

## Seismic Facies and the Onlap Index

Simulations for cases 1 and 2 use constant sediment input and subsidence and differ only in the initial basin topography. However, the resulting stratigraphic geometries are quite different; they resemble the convergent thinning ( $C_t$ ) and convergent baselapping ( $C_b$ ) seismic facies (Prather et al., 1998). The models described here suggest that these stratal patterns are the result of the interplay between subsidence and sedimentation. Stratigraphic surfaces in minibasins can have varying degrees of convergence and onlap, and the  $C_t - C_b$  seismic facies classes are best viewed as end members. Perfect onlap without any convergence occurs when there is no subsidence during one time step, the previous depositional surface remains horizontal, and the new surface must extend beyond the previous deposit and onlap the basin margin. Perfect convergence results when the onlap points do not move relative to each other, because  $V_{dep} = \eta_w \Delta t$ . There is a continuum of onlap-convergence combinations between these end members.

A way to quantify this continuum is to consider an onlap index (OI): the difference between the volumetric rate of deposition ( $Q_{in}(1 + \varphi)$ ) and the

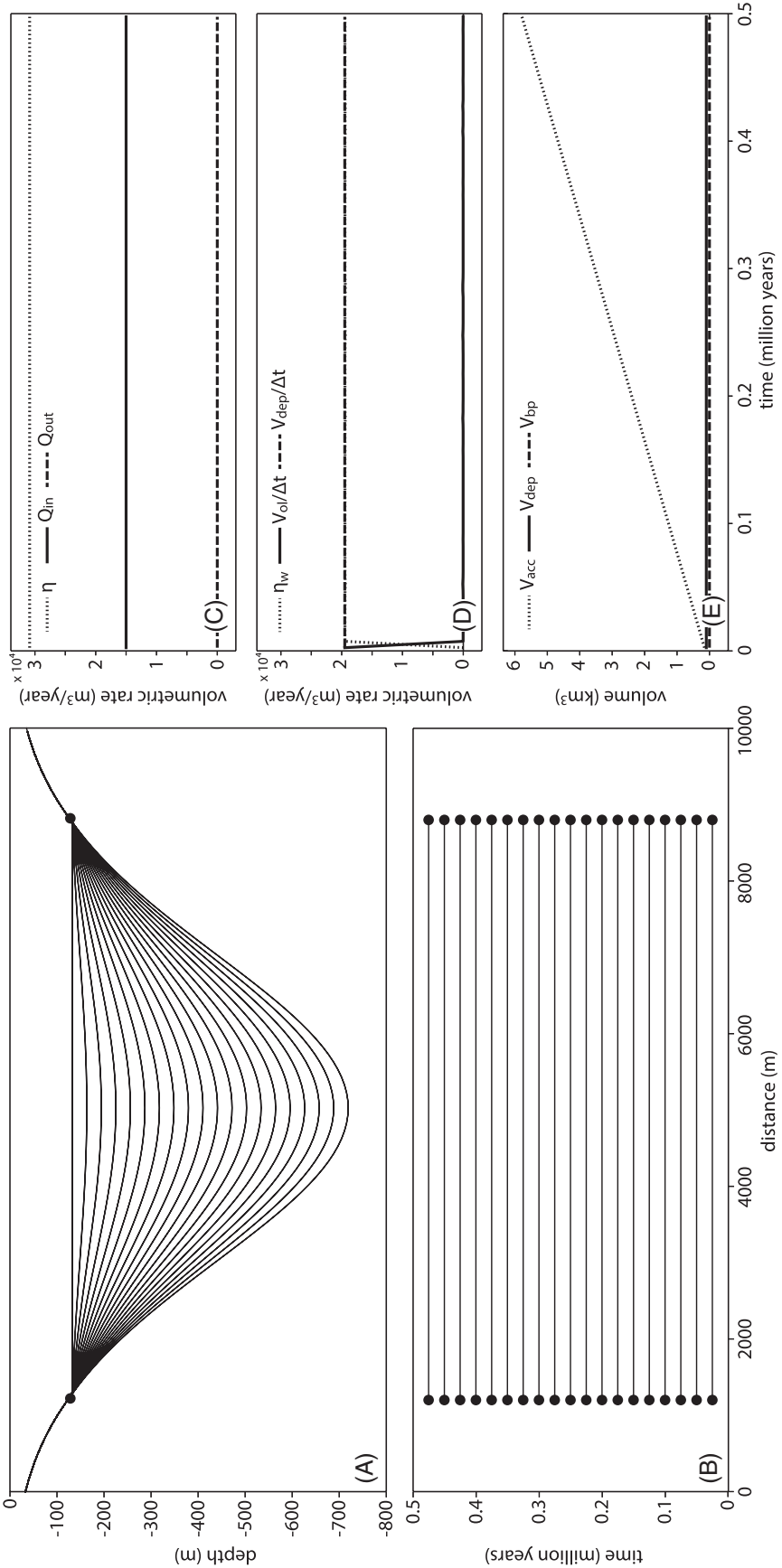


**Figure 3.** Perfect convergence occurs when all timelines converge toward the same point on the basin margin. (A) Model cross section showing stratigraphic patterns. (B) Wheeler diagram. (C, D) Plots of volumetric rates. (E) Volumes through time.

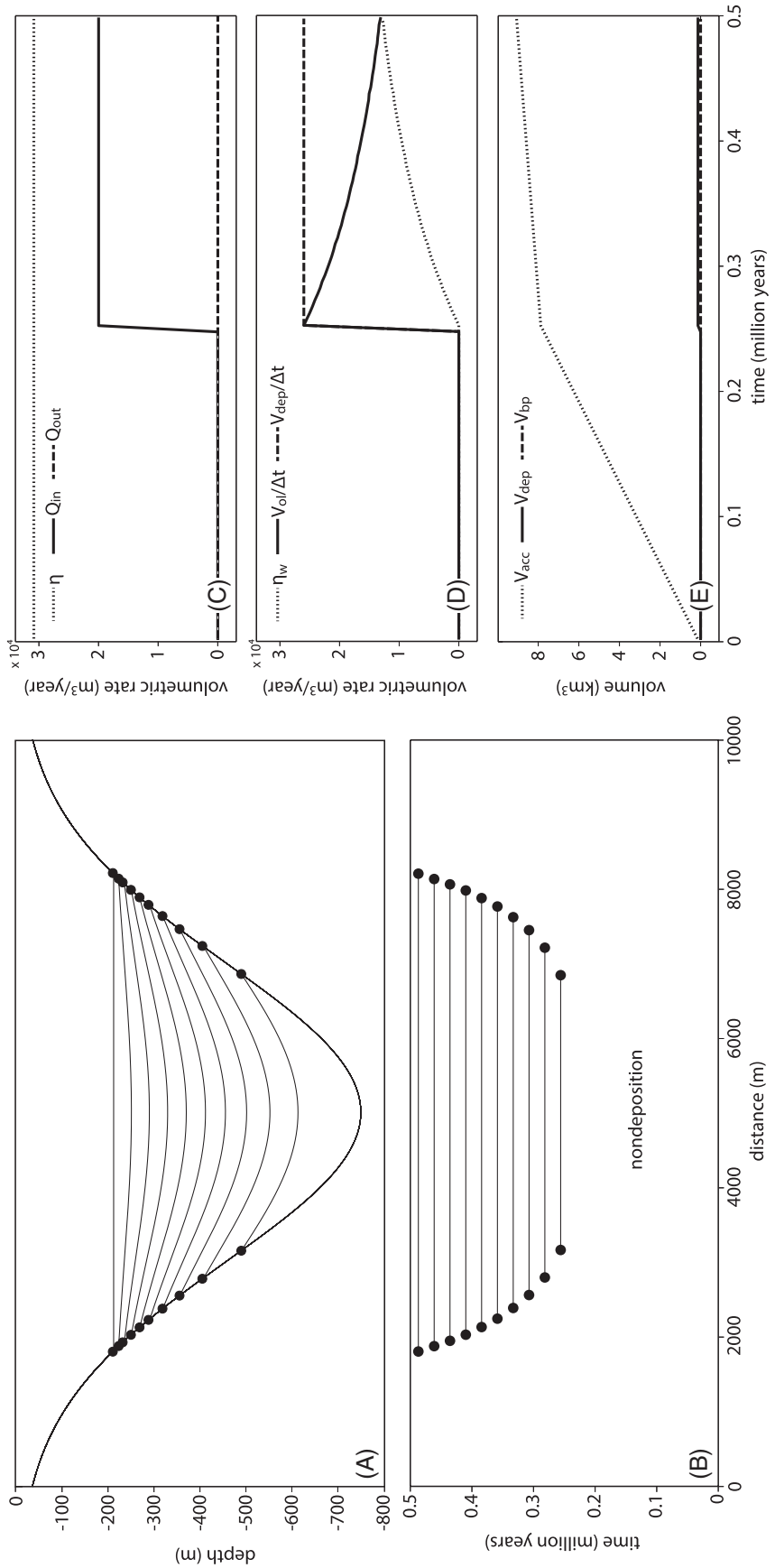


**Figure 4.** Constant sediment input entering a deep basin results in overlapping depositional surfaces. (A) Model cross section showing stratal patterns. Black dots mark the locations of onlap points. (B) Wheeler diagram. (C, D) Plots of volumetric rates. (E) Volumes through time.

volumetric subsidence rate calculated over the area of the previous deposit ( $\eta_w$ ), normalized by  $Q_{in}(1 + \varphi)$ :

$$OI = (Q_{in}(1 + \varphi) - \eta_w)/Q_{in}(1 + \varphi) \quad (3)$$

or

$$OI = 1 - \eta_w/Q_{in}(1 + \varphi) \quad (4)$$

Considering equation 1, this is equivalent to

$$OI = 1 - \eta_w(i)\Delta t/V_{dep}(i) \quad (5)$$

When there is no subsidence,  $\eta_w$  is 0, and the OI is 1. If  $\eta_w$  matches exactly the deposit volume, all surfaces converge toward the same point (or line in three dimensions) and the OI is 0. The OI can have a negative value if the pinchout points move toward the center basin relative to the previous deposit edge, that is, during the formation of offlap, defined here as the progressive updip termination of strata against an overlying surface (Figure 2C). This definition and process of formation for offlap are consistent with those described in Christie-Blick (1991) and illustrated in figure 7C of the same paper. Without normalization, the quantity  $(Q_{in}(1 + \varphi) - \eta_w)\Delta t$  is called the onlap volume ( $V_{ol}$ , Figure 2B, C). As in the case of OI, changes in the sign of  $V_{ol}$  mark changes in the migration direction of the pinchout points relative to the basin center and switches between onlapping and offlapping stratigraphic patterns.

Well-developed onlap (or  $C_b$  seismic facies) is generated when the basin already has significant relief at the beginning of sedimentation. This situation can occur when little or no sediment gets into the basin over a relatively long time period, but subsidence is active. Such periods with low sediment input correspond to condensed sections. If the background sedimentation rate (Figure 2) is set to nonzero, condensed sections are represented by thicker lines in the model plots, and their thickness is indicative of the duration of the low-sediment-input period.

### Case 3: Variable Sediment Input with No Bypass

Now that we have a better understanding of the difference between the end-member convergence and

onlap cases, we can turn our attention to more complex scenarios. In this section, we explore the effect of a sinusoidally varying sediment input coupled with constant subsidence rate. The rate of sediment supply does not exceed the accommodation available, so all the sediment is deposited within the basin and there is no bypass at any time.

The three sinusoidal sediment input cycles result in three well-defined stratigraphic packages in the basin that are separated by onlap and offlap surfaces (Figure 5A, B). In addition to being marked by stratal termination points, these surfaces also correspond to periods of reduced sediment input, that is, to condensed sections.

As discussed before, positive values of the onlap volume ( $V_{ol}/\Delta t$ , Figure 5D) correspond to stratigraphic intervals with onlap, whereas negative  $V_{ol}$  values mark intervals with offlap. The duration of the offlap is shorter than that of the onlap, because the onlap pattern keeps forming even when the sediment input has started to decrease (Figure 5D). In addition, the termination points that form during offlap are more difficult to identify because of the lower angles between stratigraphic surfaces compared to the onlap angles. This difference in stratal angles and the limited thickness of the section with offlap (Figure 5A) might be the reasons why offlapping stratigraphic patterns are rarely seen in seismic data coming from minibasin fills.

Because the rate of sediment input is always variable in this scenario, none of the pinchout points falls in exactly the same place and there is no perfect convergence.

### Case 4: Stratigraphy of Basins with Bypass

If we keep all the model parameters the same as in the previous section but double the rate of sediment input, the sediment supply will periodically exceed the accommodation and there will be significant sediment bypass (Figure 6). Although subsidence is constant in time and the sediment input cycles are symmetric, the stratigraphic cycles of the basin fill are asymmetric: sections corresponding to times of sediment bypass (dashed lines in Figure 6A, B) always overlie ponded sections with well-developed onlap geometries. These in turn are underlain by

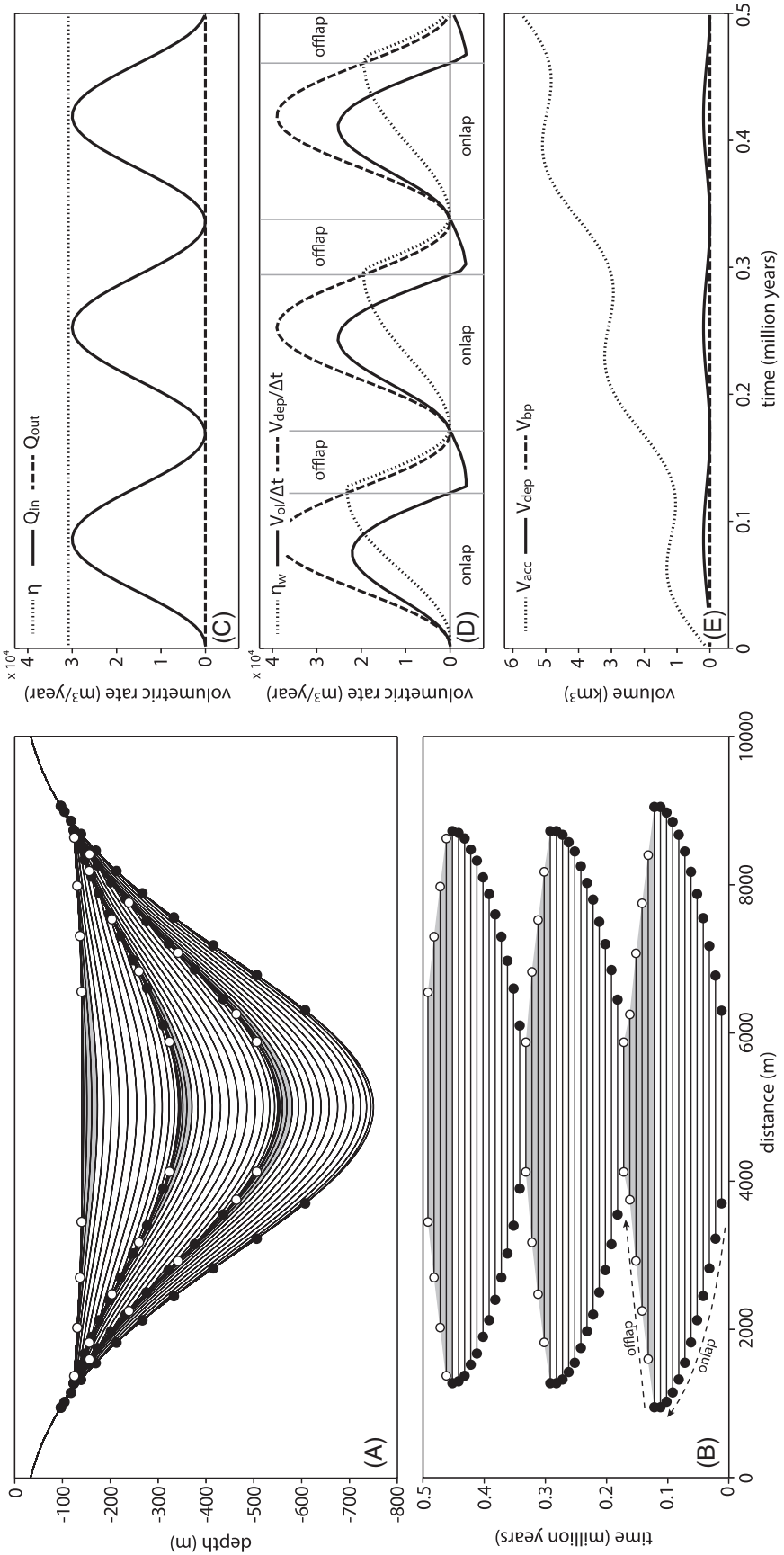


**Figure 5.** (A) Basin cross section showing model output with three sinusoidal cycles of sediment input and constant subsidence, without bypass. (B) Wheeler diagram of cross section shown in (A). Black dots mark termination points that step toward the basin margin (onlap); white dots correspond to termination points that move toward the basin center (offlap). Intervals with offlap are shown with gray shading. (C, D) Plots of volumetric rates. (E) Volumes through time.

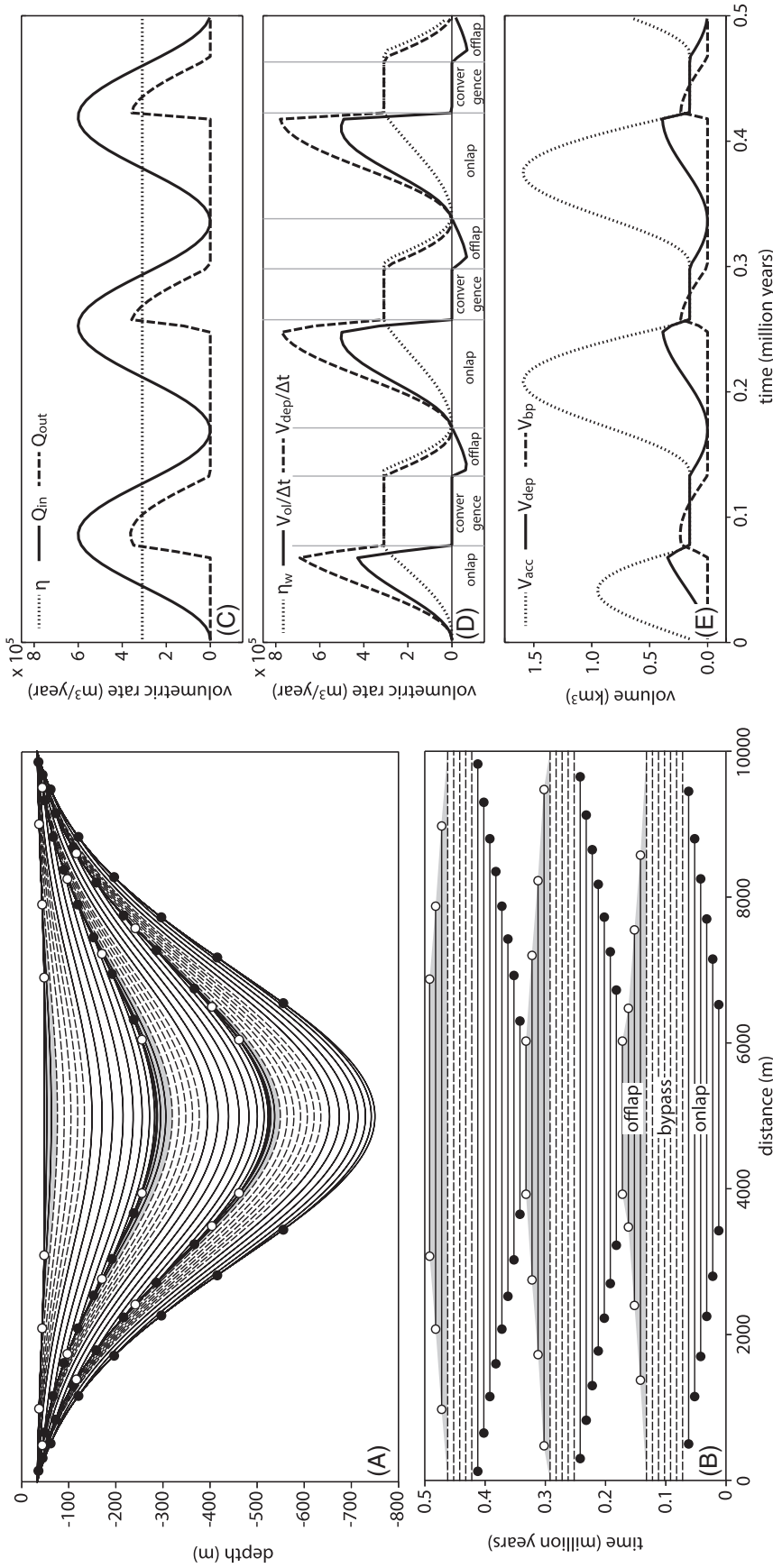


**Figure 6.** (A) Basin cross section showing model output with three sinusoidal cycles of sediment input and constant subsidence, with bypass. Black dots mark termination points that step toward the basin margin (onlap); white dots correspond to termination points that move toward the basin center (offlap). Intervals with offlap are shown with gray shading. (B) Wheeler diagram. (C, D) Plots of volumetric rates. (E) Volumes through time.

condensed sections, marked in the model output by the high density of time lines. The cyclicity of the sediment input curves ( $Q_{in}$ ) does not need to be sinusoidal; stratigraphic cycles comparable to those shown in Figure 6 develop with any pattern of episodic changes in sediment input.

During time steps with sediment bypass, stratigraphic surfaces terminate at the basin edge, and the bypass package has a convergent character (Figure 6A, D). However, times of bypass are usually also times of significant erosion and development of channel systems in the basin, particularly near the basin exit area, and these processes are not represented in the model. In nature, the seismic intervals that correspond to periods of bypass commonly show a chaotic character instead of a convergent thinning geometry (Prather et al., 1998; Booth et al., 2003).

Stratigraphic cycles that consist of a condensed section followed by  $C_b$  seismic facies and a bypass-related unit at the top have been described from some of the well-known minibasins in the Gulf of Mexico, such as the Auger (Booth et al., 2003) and Mars basins (Meckel et al., 2002).

### **Case 5: Variable Subsidence Rate, Constant Sediment Input**

In the models discussed so far, we assumed that sediment discharge varies significantly through time, whereas subsidence stays constant or decreases linearly. This is reasonable because salt-withdrawal minibasins commonly experience fluctuations in sediment supply, as feeder channels are abandoned or reactivated.

It is tempting to think that a changing subsidence rate would have a similar effect on stratigraphic architecture to that of changing the sediment supply. For example, would a constant sediment input coupled with a sinusoidally varying subsidence result in the same stratigraphic architecture as constant subsidence and variable sedimentation rates (Figures 5, 6)? Figure 7 shows the result of a simulation with three cycles of decreasing-to-increasing subsidence and constant sediment input. In contrast with the constant subsidence scenario, where condensed sections coincide with a basin-wide onlap surface (Figures 5, 6), unconformities in this case are restricted to the

basin margins, and they form exactly when the basin center experiences the largest rates of sedimentation (Figure 7A). When subsidence is at a maximum, the onlap points are located closer to the basin center; then they move outboard as there is less space to accommodate all the incoming sediment in the central part of the basin. The volumetric onlap curve and the subsidence calculated over the depositionally active area are  $90^\circ$  out of phase (Figure 7D).

Although this scenario is unlikely in salt-withdrawal minibasins with passive diapirism, episodic deformation with a background of relatively constant sediment supply can occur at basin margins affected by tectonic shortening. In this case, the modeling results shown here highlight that such basin-margin unconformities do not correspond to basin-center unconformities and condensed sections; instead, they correlate with expanded sedimentary sections in the center of the basin.

### **Case 6: Subsidence Rate and Sediment Input Both Variable and Out of Phase**

It is possible that subsidence rate is variable through time and its variation is driven by sediment loading. If there was no lag time between the sediment input curve and the subsidence curve (i.e., if the salt substrate instantaneously responded to loading), and the two curves were perfectly in phase, the result would be a stack of perfectly convergent sequences (not shown here), separated only by condensed sections, but no onlap or offlap surfaces.

However, if we assume that there is a lag time between the sediment loading and the change in subsidence rate, the results are more intriguing. If the two curves are  $90^\circ$  out of phase, the basin fill has some well-defined depositional sequences (Figure 8). Although the onlap surfaces are better developed in this case, in real data sets it would be difficult to distinguish this scenario from one where the subsidence rates are less variable (Figure 5).

### **Case 7: Sediment Input as a Step Function**

Another question worth investigating is whether our choice of sinusoidally varying sediment input has a

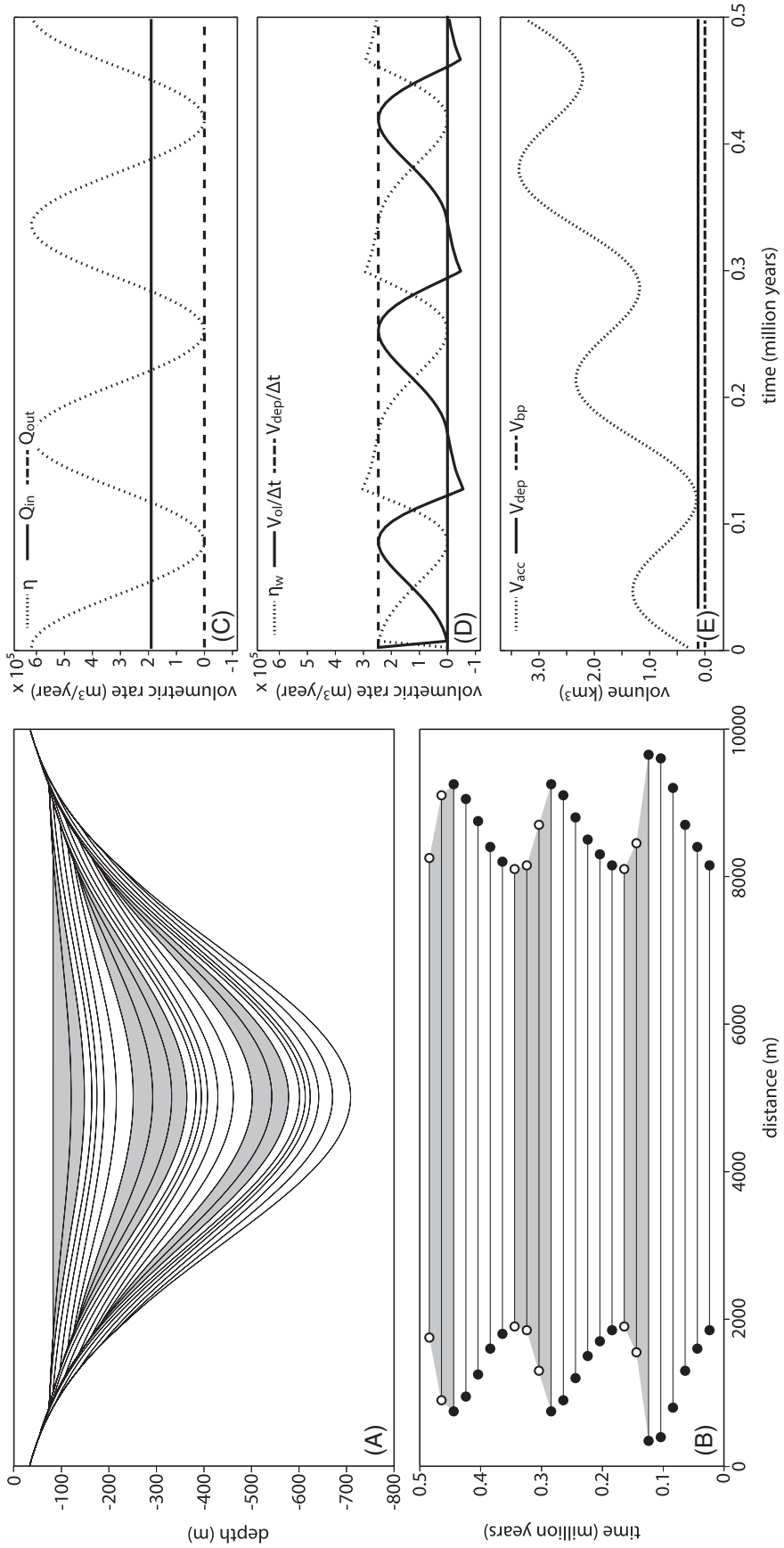


**Figure 7.** (A) Cross section of model with constant sediment input and sinusoidally varying subsidence. (B) Wheeler diagram. (C, D) Plots of volumetric rates. (E) Volumes through time.

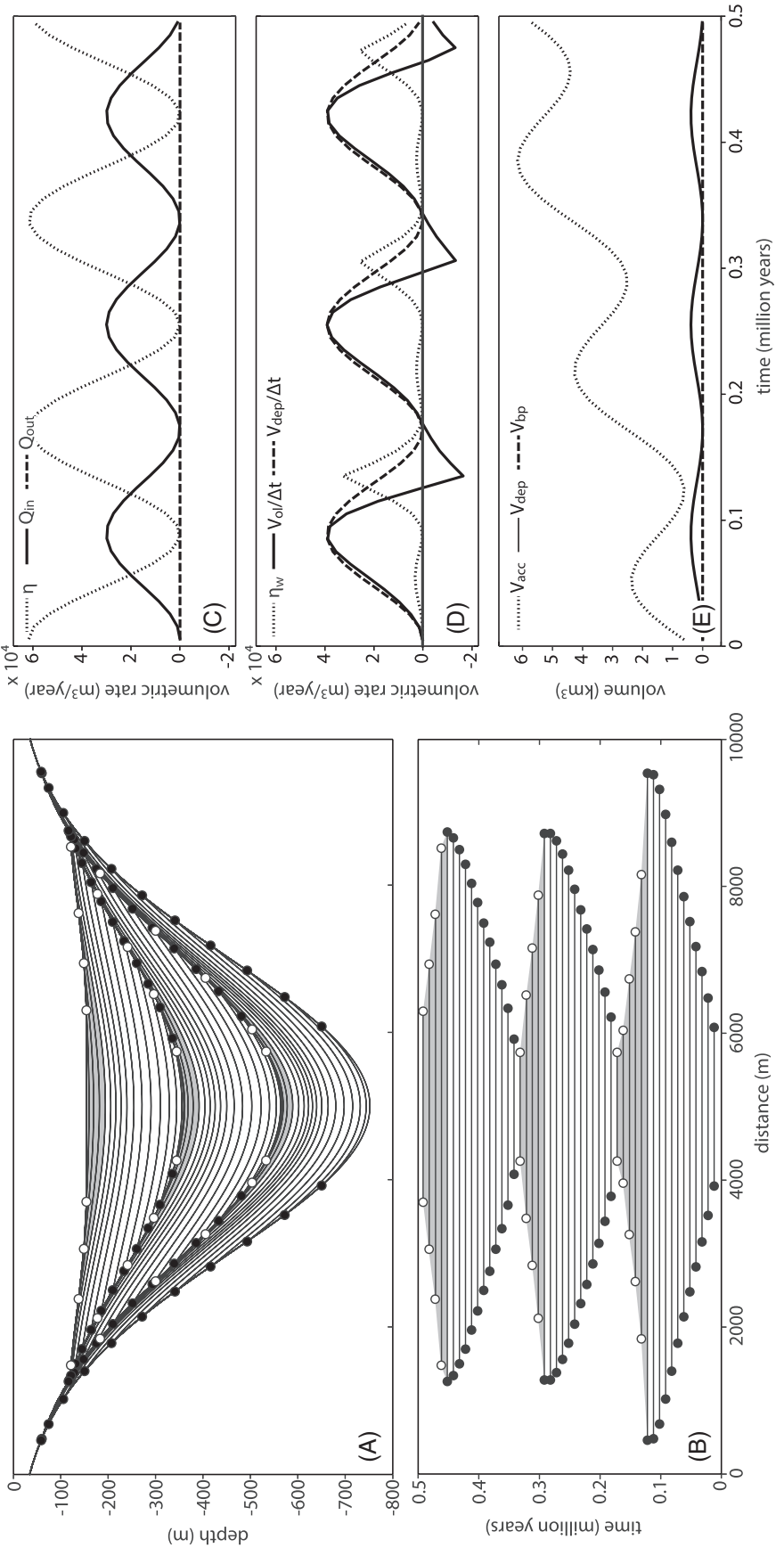


**Figure 8.** (A) Cross section of model with sinusoidally varying sediment input and sinusoidally varying subsidence; sediment input and subsidence are out of phase. (B) Wheeler diagram. (C, D) Plots of volumetric rates. (E) Volumes through time.

significant impact on the geometry of the deposits. As changes in sediment supply to minibasins are likely to be driven by distinct events such as channel avulsions and delta lobe abandonments, it is possible that it is more appropriate to model changes in sediment supply as a step function: sediment input is either turned on or it is off. Keeping subsidence rate constant and letting sediment input vary in primez results in one depositional sequence for each interval with large sediment input (Figure 9). In contrast with models that use a sinusoidally varying sediment input, there is no offlap in this case because sediment supply is never decreasing progressively; instead, it quickly drops to zero. In fact, the on-off sediment supply model has been successfully used to reproduce the large-scale geometries of Brazos-Trinity Basin 4 (see case 8). The common occurrence of on-off sediment input patterns in minibasins might be another reason why offlap geometries are rarely observed in slope basins.

### **Case 8: Static Fill-and-Spill: Linked Basins with No Subsidence**

Using the model described here, it is possible to simulate deposition across multiple linked basins by setting the input sediment function of the downdip basin to the bypass sediment curve that comes from the updip basin. In the next two cases, we explore two relatively simple scenarios: one with no subsidence during sedimentation, and the other with subsidence added.

The idea of intraslope basin deposition happening in a fill-and-spill style goes back to early studies of the California Borderland (Gorsline and Emery, 1959). According to the conventional, static fill-and-spill model, which assumes that basin accommodation already exists at the beginning of sedimentation and there is no subsidence during deposition, basins located updip on the slope have to be filled first, before those further down the slope (Satterfield and Behrens, 1990; Prather et al., 1998; Beaubouef and Friedmann, 2000; Sinclair and Tomasso, 2002). However, using a high-resolution chronostratigraphic data set, Pirmez et al. (2012) showed that the minibasin fills of the Brazos-Trinity system in the western Gulf of

Mexico do not conform to this static spill-and-fill model, probably because the subsidence rates were large enough to create significant new accommodation during condensed section deposition, yet not large enough to prevent sediment from abruptly propagating through all basins during times of high sediment supply.

To illustrate the difference between the static and dynamic versions of the spill-and-fill model, we first look at deposition across two linked basins of the same size during three step-like sediment input cycles and no subsidence. The resulting basin fills are almost entirely different in age, apart from the condensed sections that are deposited in both basins at the same time, as illustrated by the chronostratigraphic diagram (Figure 10). The first two condensed sections in basin 1 correlate to the basal condensed section in basin 2.

### **Case 9: Dynamic Fill-and-Spill: Linked Basins with Subsidence**

In the second scenario with two linked basins, we keep all input parameters the same as in case 8, but there is no significant basin relief in either of the basins at the beginning of sedimentation, and there is constant subsidence in both basins during model evolution. The resulting basin fills are essentially coeval at the scale of the whole section (Figures 11, 12), an overall age relationship that is quite different from that of the static fill-and-spill case (Figure 10). Fill-and-spill is still present, but it is happening at a finer temporal scale, that is, at the scale of individual sediment input cycles. This is possible because the basin relief never gets too large during condensed section deposition, and sediment is able to spill into basin 2 during all three periods of high sediment input. The fine-scale age differences between individual cycles in the two basins are likely to be below the resolution of the available age dating methods (Pirmez et al., 2012).

Although static fill-and-spill (case 8) is clearly a possibility—for example, any of the relatively deep basins that are visible on the present-day seafloor in the Gulf of Mexico would have to be filled first to the spillpoint before deposition could

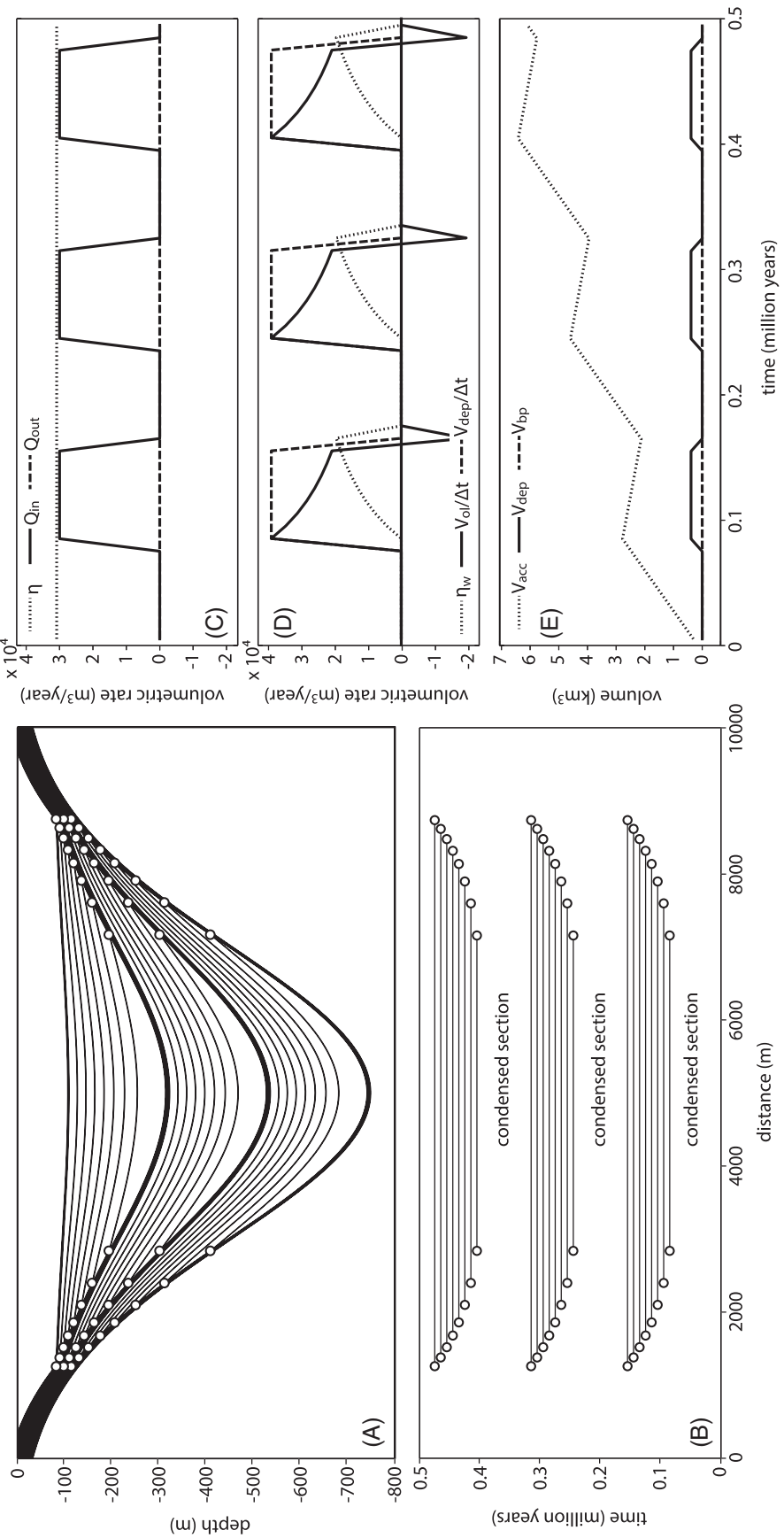


**Figure 9.** (A) Cross section of model with on-off sediment input and constant subsidence. (B) Wheeler diagram. (C, D) Plots of volumetric rates. (E) Volumes through time.

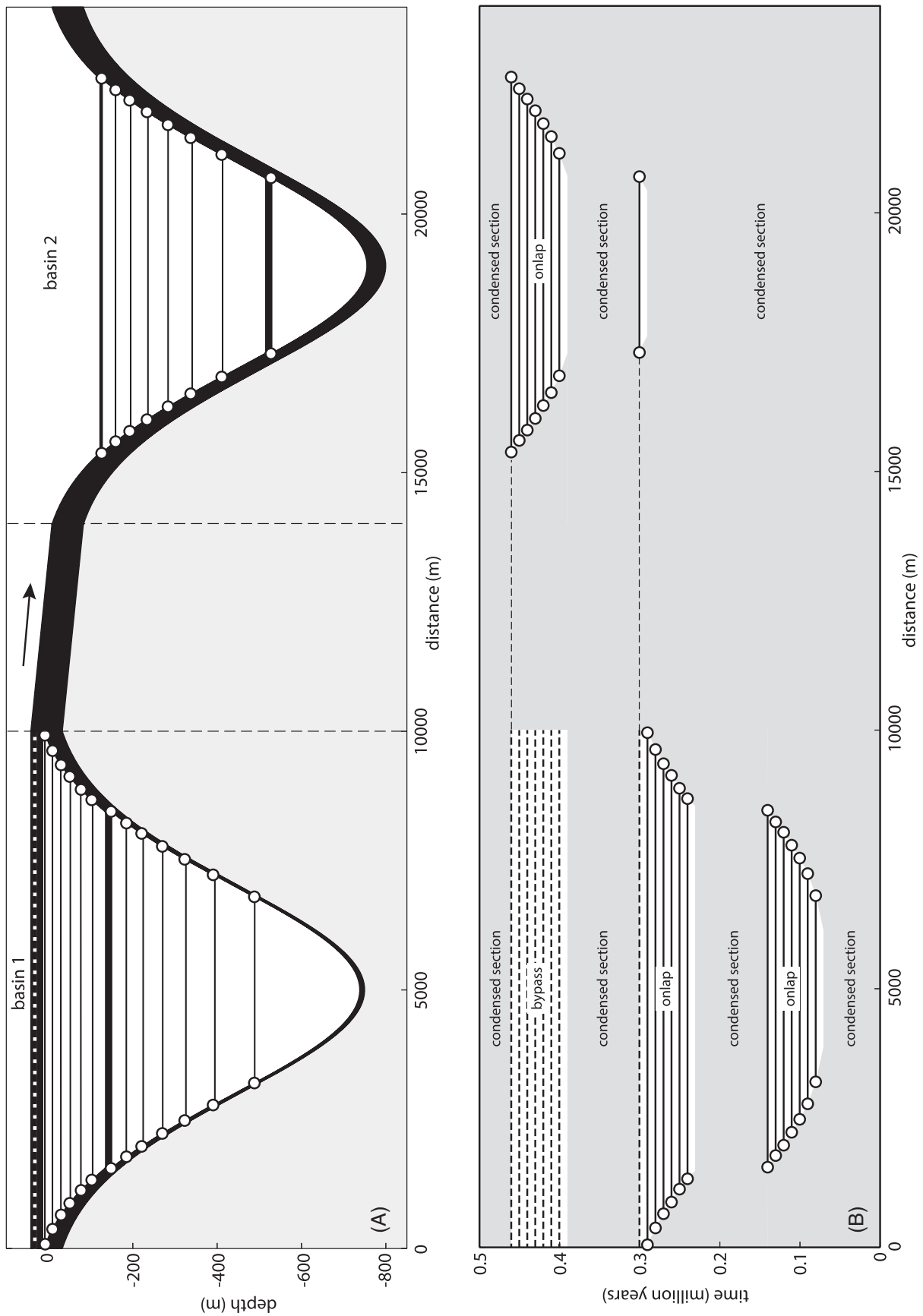


**Figure 10.** The classic fill-and-spill model illustrated with two linked basins, three step-like sediment input cycles, and no subsidence during sedimentation. The updip basin fill is older than the deposits in the downdip basin.

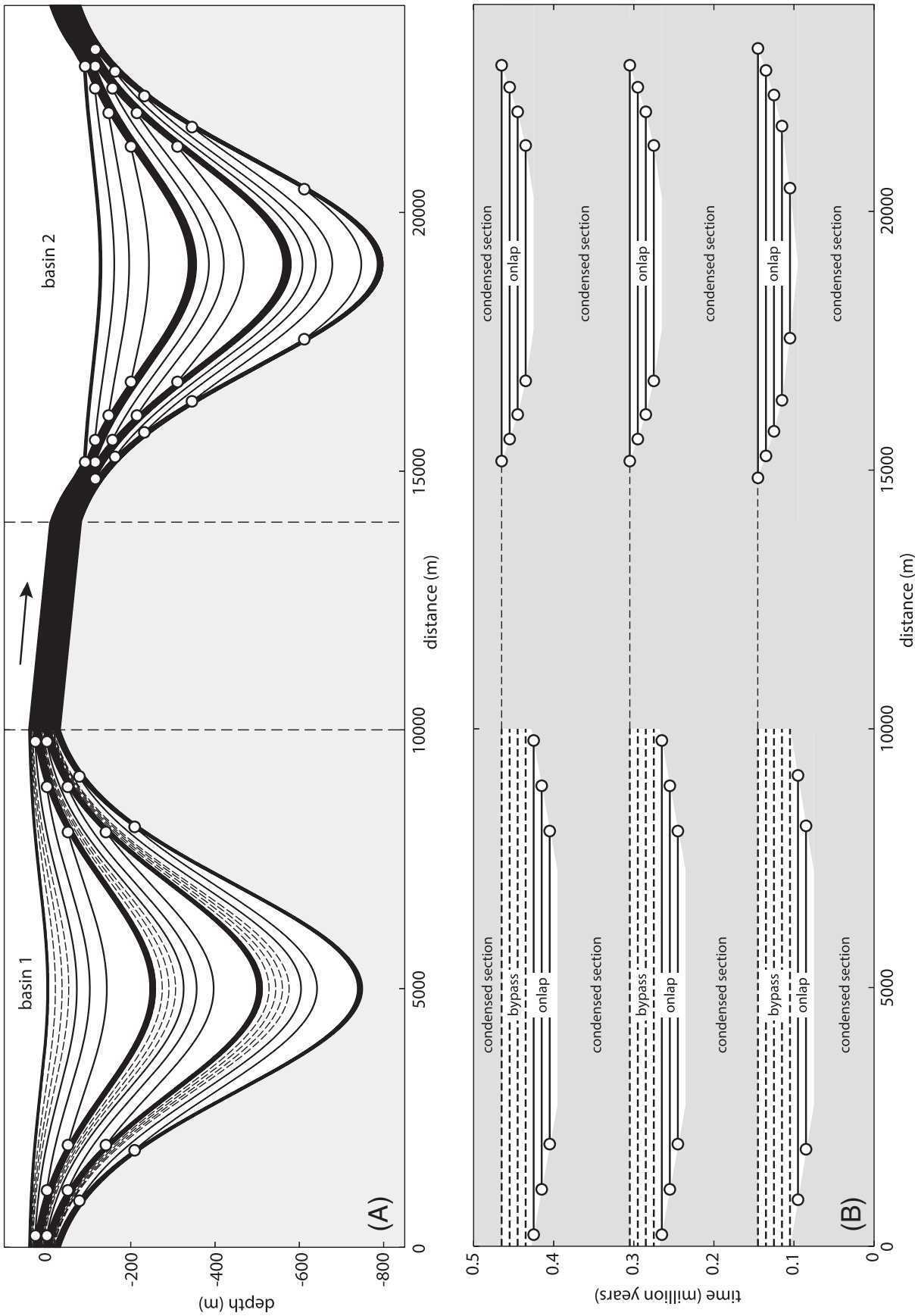


**Figure 11.** If subsidence is taking place in parallel with sedimentation, the fill-and-spill cycles are of shorter duration and the basin fills are largely coeval. Apart from the constant and nonzero subsidence function, same input parameters as for model shown in Figure 10.

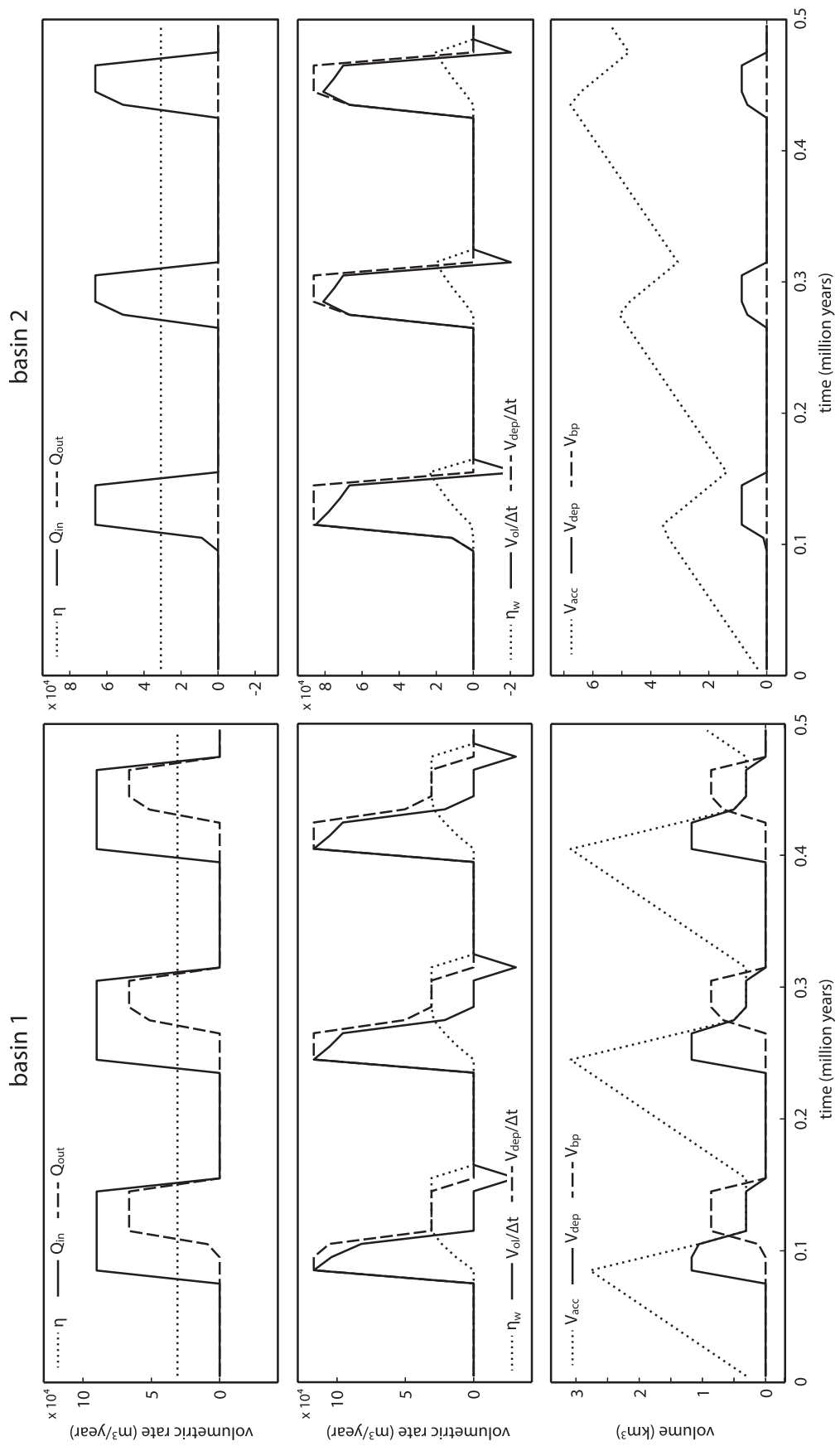


**Figure 12.** Plots of volumetric rates and of volumes as a function of time for the two basins shown in Figure 11.

proceed further downdip (Figure 1)—there is evidence that many linked basin systems go through repeated fill-and-spill cycles at a smaller scale and a higher temporal frequency (Booth et al., 2000; Pirmez et al., 2012).

## APPLICATIONS TO INTRASLOPE BASINS IN THE GULF OF MEXICO

### Case 10: Brazos-Trinity Basin 4

The Brazos-Trinity source-to-sink system is located in the northwestern Gulf of Mexico, with four linked salt-withdrawal intraslope minibasins receiving most of the sediment delivered to the continental slope by the Brazos and the Trinity Rivers (Winker, 1996; Badalini et al., 2000; Beaubouef and Abreu, 2006; Mallarino et al., 2006; Pirmez et al., 2012; Prather et al., 2012b; Figure 13). Basin 4 is a relatively deep depression that forms the final sink at the distal end of the system; no sediment is getting out and further down the slope from Basin 4 (Figure 13). As a result, the basin fill is not affected by sediment bypass and it provides an opportunity to understand how stratigraphic packages with different degrees of convergence and onlap can develop in such settings.

Recent work on the high-resolution chronostratigraphy of the Brazos-Trinity system shows that the three condensed sections penetrated by Integrated Ocean Drilling Program well U1320 (Figure 14A) comprise most of the time recorded by the basin fill (Pirmez et al., 2012). The two stratigraphic units bounded by these condensed sections consist of turbidites sourced from updip and slump deposits derived from the basin margins. The older of these stratigraphic units was deposited during marine isotope stage 5, with a relatively low volumetric sediment flux of approximately  $40,000 \text{ m}^3/\text{yr}$  ( $1,412,587 \text{ ft}^3/\text{yr}$ ); the younger, thicker package includes series 40, 50, and 70 of Pirmez et al. (2012) and was deposited during the last glacial lowstand (marine isotope stage 2), with a much larger average sediment flux of approximately  $1,000,000 \text{ m}^3/\text{yr}$  ( $35,314,677 \text{ ft}^3/\text{yr}$ ) (Figure 14). In addition to these parameters, our model assumes that Basin 4 had only limited topographic relief at the beginning of deposition of the first condensed section and that the basin center

had a constant subsidence rate of  $0.1 \text{ mm/yr}$  ( $0.004 \text{ in./yr}$ ), with zero subsidence around the edge. This rate is consistent with the idea that the observed curvature of the present-day basin floor has formed during the last 16,000 yr, a time of no coarse clastic sediment input and condensed section deposition in Basin 4. The basin shape is approximated with a 15 km (9 mi) wide elliptic paraboloid.

Our minibasin model (Figures 14, 15) captures well the key differences between the lower and upper stratigraphic packages visible in the seismic section (Figure 14A): the lower unit shows strong convergence and poorly defined onlap, in contrast to the upper package, which has almost no convergence and well-defined onlap geometries at the basin edge. These stratal patterns are similar to the  $C_t$  and  $C_b$  facies of Prather et al. (1998) and they are the result of (1) ongoing subsidence during sedimentation; (2) intermittent sedimentation: long periods of no significant siliciclastic input interrupted by relatively short phases of high sediment flux; and (3) periods of overall high sediment flux having a wide range of sedimentation rates: the upper package has a sediment flux 25 times larger than the lower one.

### Case 11: Auger Basin

Numerous intraslope basin fill successions are many times thicker (up to thousands of meters thick) than the fill of Basin 4 of the Brazos-Trinity system, described and modeled in the previous section. Significant parts of these basin fills show evidence of sediment bypass into the downdip basin(s). At a large scale, the bypass zones tend to be concentrated within the upper part of the basin fill; this section has been described as the bypass facies assemblage, in contrast with the underlying ponded facies assemblage (Prather et al., 1998; Booth et al., 2003). The Auger Basin in the Gulf of Mexico is a good example: convergent baselapping ( $C_b$ ) seismic facies dominates the lower part of the basin fill; this is overlain by a package with numerous chaotic seismic units that correspond to overall more channelized, bypass-related deposits (Booth et al., 2003; Figure 16A).

This overall transition from sediment ponding to increasing bypass likely reflects the long-term filling

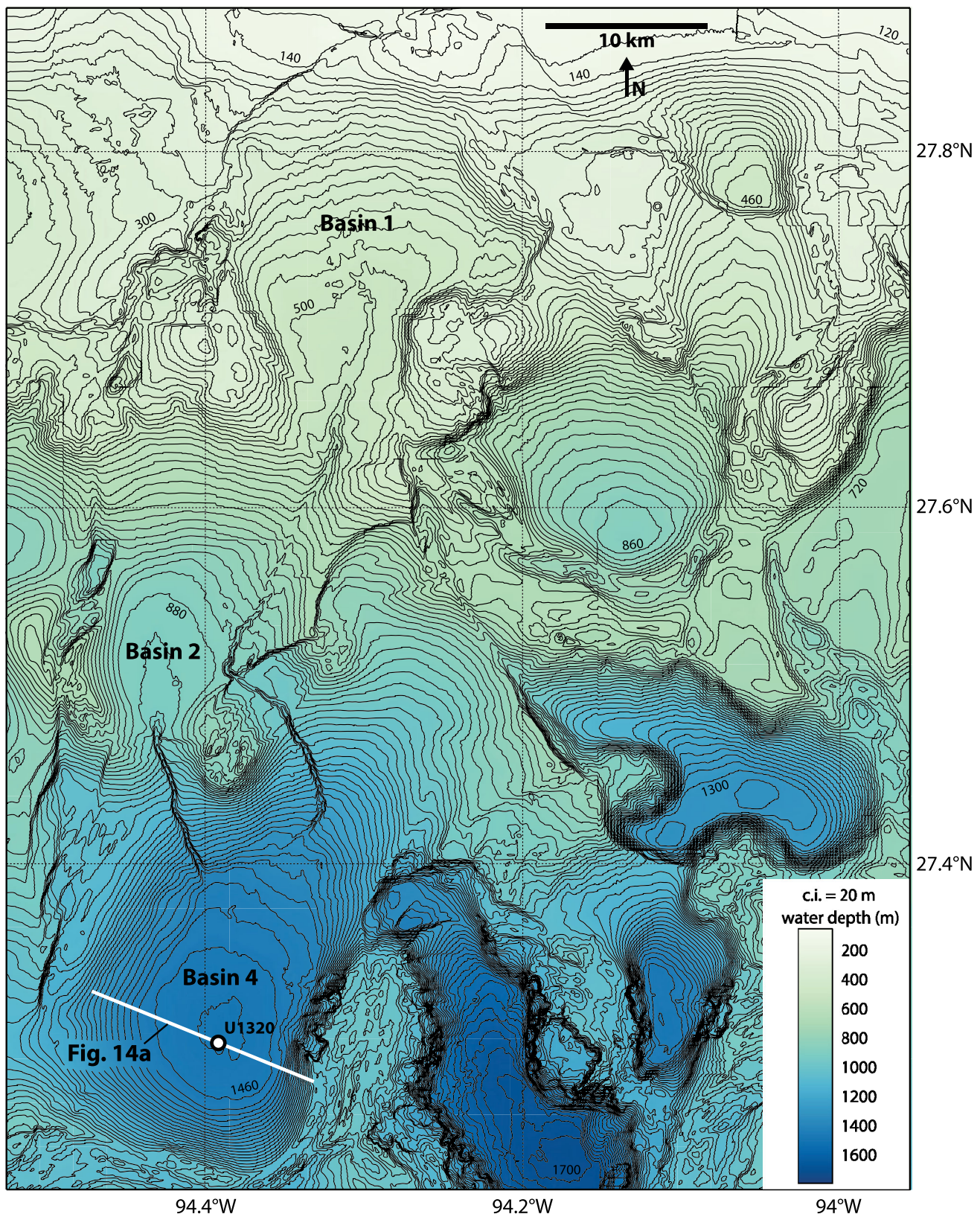


**Figure 13.** Bathymetric map of the upper slope in the northwestern Gulf of Mexico. Basins 1, 2, and 4 of the Brazos-Trinity system and location of Integrated Ocean Drilling Program well U1320 are shown.

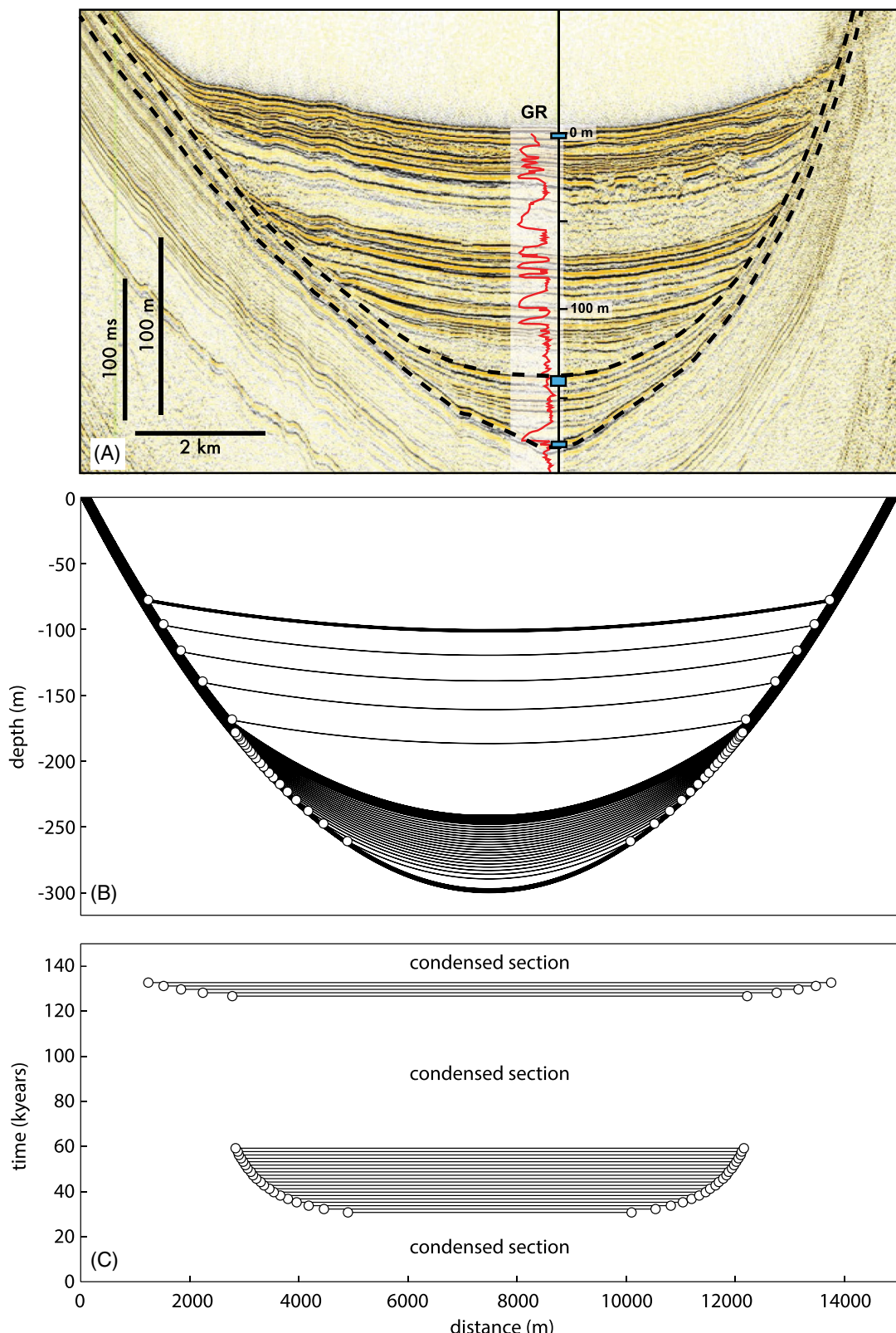
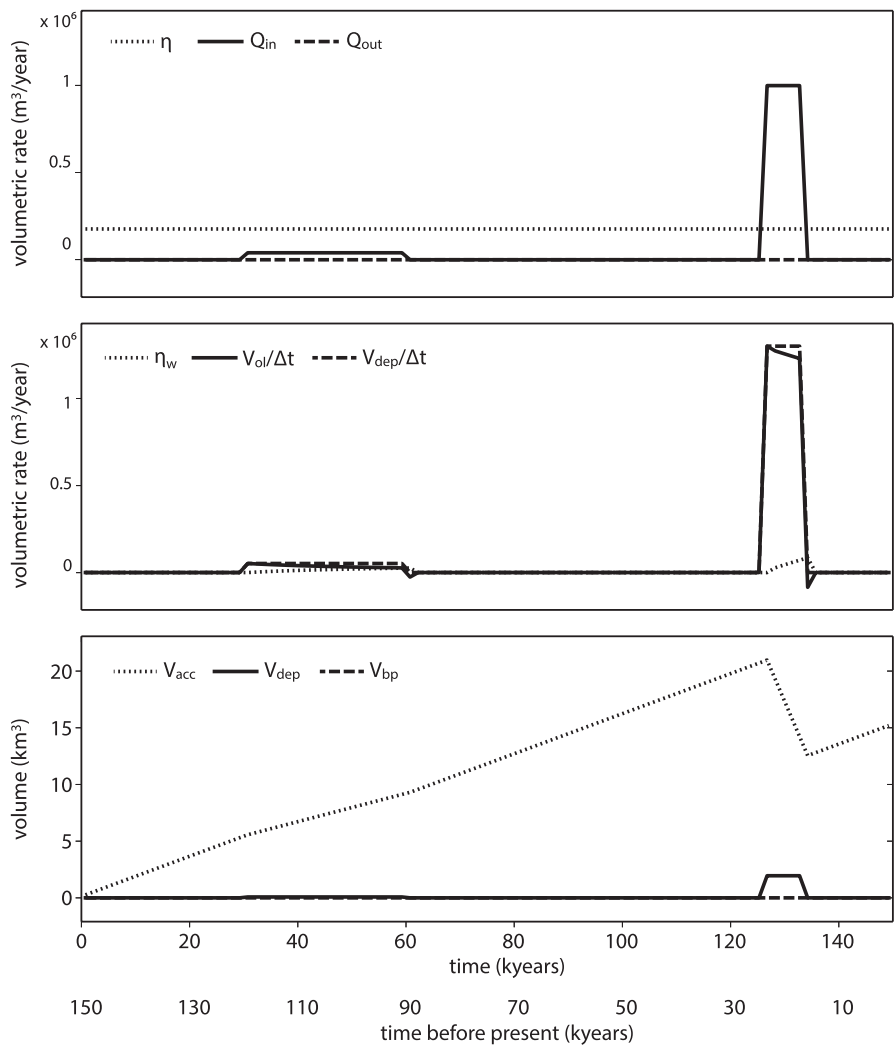


**Figure 14.** (A) High-resolution seismic reflection profile across the distal part of Brazos-Trinity Basin 4. Gamma-ray (GR) curve in the middle of the basin is from Integrated Ocean Drilling Program research well U1320 (see Pirmez et al., 2012, for more details). Locations of condensed sections in the well are indicated with rectangles. (B) Cross section of model for Brazos-Trinity Basin 4. (C) Wheeler diagram.

**Figure 15.** Plots of volumetric rates and volumes through time for the model shown in Figure 14.



of the basin. However, this process was not a simple, static fill-and-spill (e.g., Sinclair and Tomasso, 2002). Intervals with strong evidence for bypass are present within the ponded facies assemblage as well, and the curved and convergent nature of reflection packages suggest that subsidence was active during deposition (Figure 16A). A plausible explanation for the gradual transition from ponding to bypass is a decline over time in subsidence rate. This could be the result of decreasing salt thickness below the basin center; as the thickness of underlying salt drops, the flow rate decreases as well.

A model run with spatial and time parameters roughly similar to those observed in Auger Basin reproduces both the small-scale ponded-to-bypass cycles and the large-scale transition from

ponding to bypass facies assemblages (Figure 16B). Accommodation is fairly large during early basin evolution and declines during the bypass phase (Figure 17). However, even during the deposition of the lower, ponded section, the short-term sediment influx cycles cause a large enough variation in accommodation and the system can easily enter into brief periods of bypass.

## DISCUSSION

### Geometry of Deposits: Reality versus Model

The simple rigid-lid model presented here is an attempt to capture the main characteristics of large-scale stratigraphic patterns in slope minibasins. In

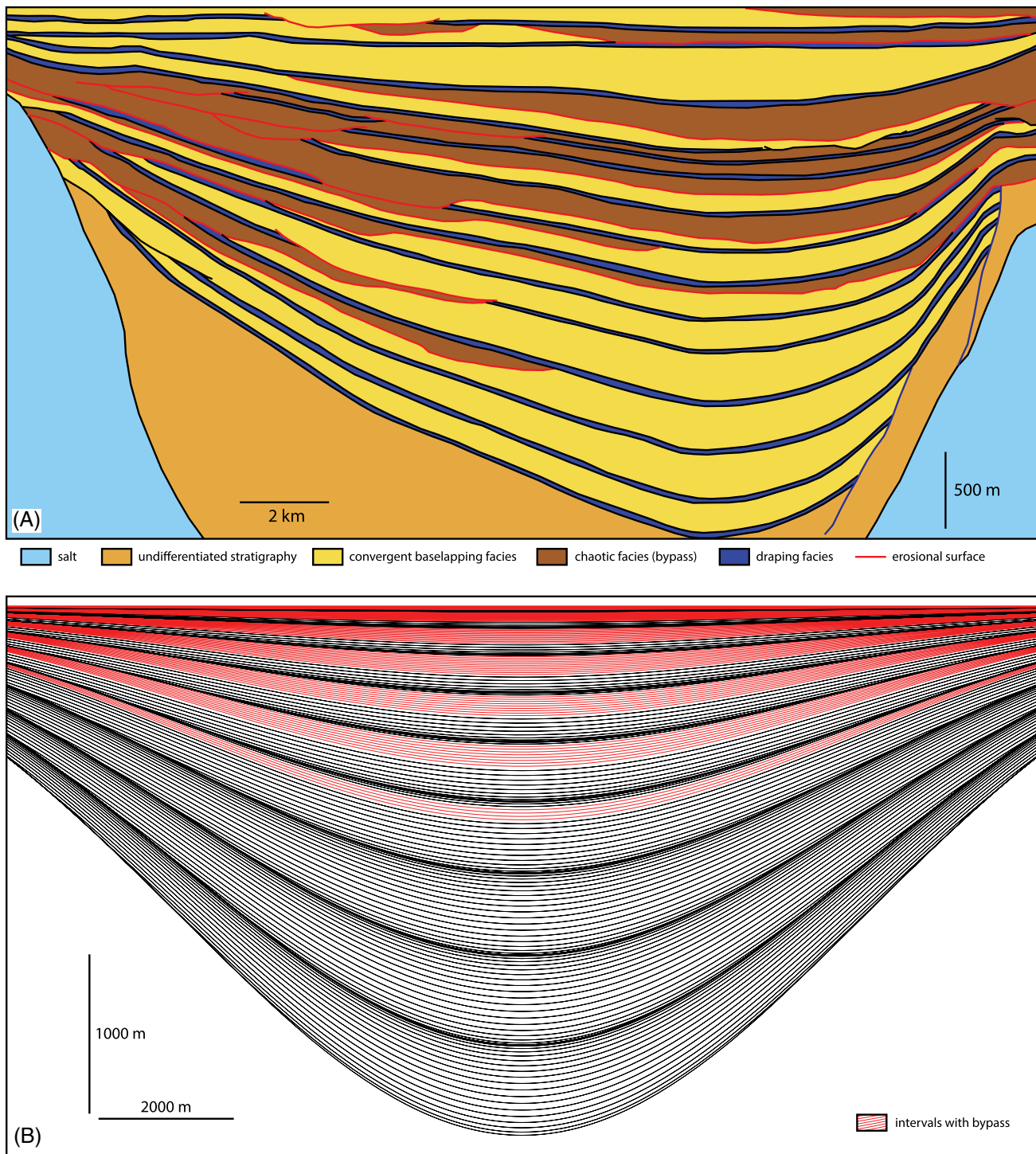
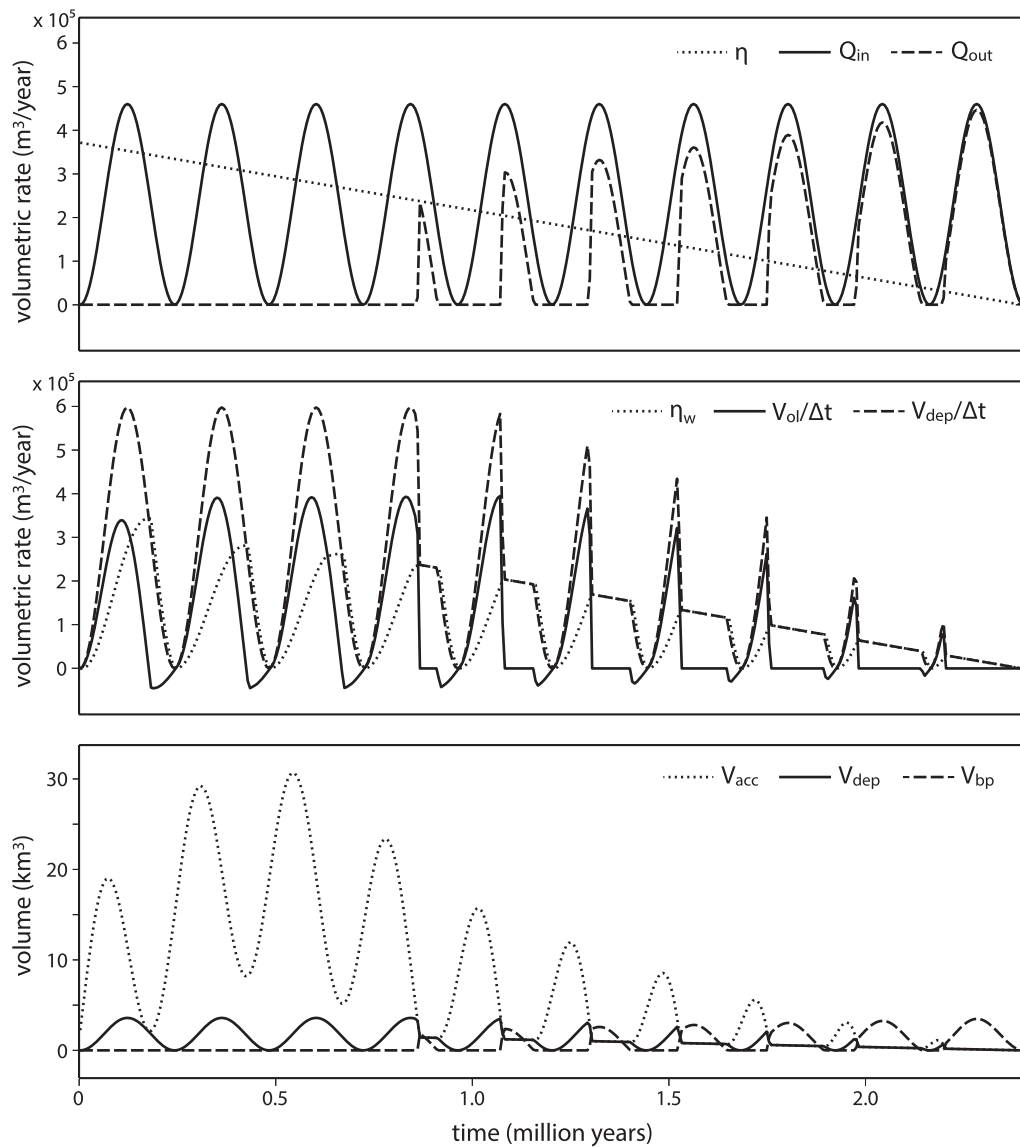


**Figure 16.** (A) Interpreted seismic facies in a cross section across the Auger Basin, Gulf of Mexico. Redrawn from Booth et al. (2003, used with permission of Elsevier). (B) Cross section of model for Auger Basin.

each time step, the thickest deposits are located exactly at the basin center, and many of these layers extend across most of the basin. In reality, with the exception of basin-floor turbidites that cover most of

the basin area, slope basin fills consist of turbidite lobes, channels, and mass transport complexes. Important processes such as compensational stacking (Lyons, 2004; Straub et al., 2009) and erosion (Booth

**Figure 17.** Plots of volumetric rates as a function of time for Auger Basin model shown in Figure 16B.



et al., 2000) are not captured by our model. However, it has been observed that at a larger scale, both shales and sands can have large lateral extents in these basins (Reilly and Flemings, 2010), and seismic units and the corresponding seismic reflections commonly extend from one side of the basin to the other (e.g., Figures 14A, 16).

The model presented here does not reproduce finer-scale reservoir heterogeneities that might influence fluid flow, such as shale drapes. Additional processes such as compensation and erosion would have to be added to start representing stratigraphic architecture at this finer scale. A compensational model of lobe stacking (e.g., Pyrcz et al., 2005; Straub et al., 2009) could be used to add more

detail and complexity to the stratigraphic model described here.

At a larger scale, more realistic basin shapes and subsidence patterns would result in a larger variety of more realistic stratigraphic patterns. Such basin shapes and subsidence maps could be extracted from three-dimensional seismic data and easily used as model inputs.

In addition to the inherent limitations of the model, it is also important to consider that similar stratigraphic geometries may have different expressions in seismic data, depending on the frequency content of the seismic image, and vice versa, the same low resolution seismic patterns may correspond to different stratigraphic architectures at a finer scale.

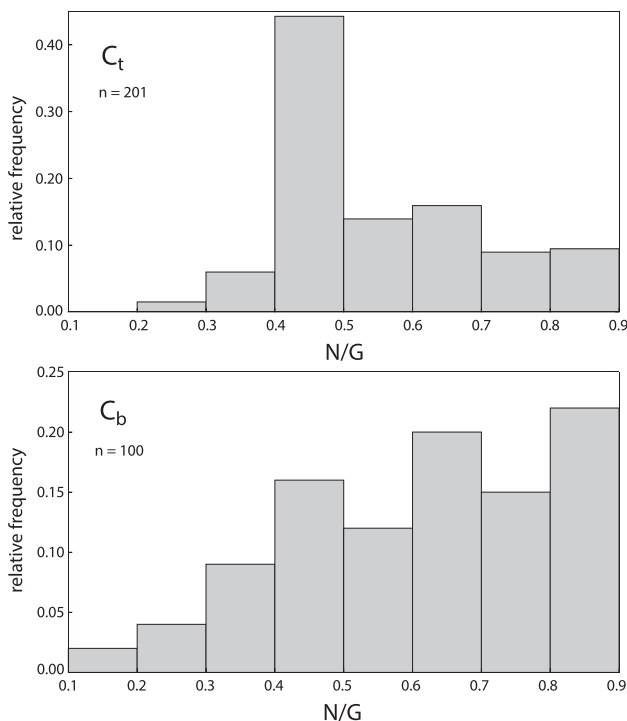


**Figure 18.** Net/gross (N/G) distributions for sand units within convergent thinning ( $C_t$ ) and convergent baselapping ( $C_b$ ) seismic facies. Replotted from Prather et al. (1998).

### Stratal Patterns and Sand Distribution

Early work on seismic facies typical of intraslope minibasins has shown that overall sand content varies by seismic facies (Prather et al., 1998). Although

there is significant variability, sandy units within high-amplitude baselapping seismic facies tend to have the highest sand fraction (Figure 18). The overall sand content is also highest in the high-amplitude baselapping facies (table 3 in Prather et al., 1998). These data suggest that depositional sequences with well-defined onlap tend to be more sand rich than those characterized by convergence and lack of onlap.

In light of the modeling results presented here, there are two potential explanations for this observation. If the subsidence rate is kept constant, the degree of convergence and the definition of the onlap pattern is influenced by the sediment input rate: as shown by the model representing Brazos-Trinity Basin 4, large sediment supply to the basin results in well-defined onlap and limited convergence, whereas low sediment supply leads to the formation of convergent packages with poorly defined onlap (Figure 14). The majority of the sand in this case does occur in the upper unit with high sediment input rates. Thus, the high sand content of the  $C_b$  facies may be because of the fact that this stratal geometry is characteristic of high sediment input rates, which in turn are prone to be sand rich.

The second possibility is that many of the convergent thinning seismic facies ( $C_t$ ) occurrences analyzed by Prather et al. (1998) come from stratigraphic intervals with bypass. Although such intervals commonly contain channel systems and chaotic

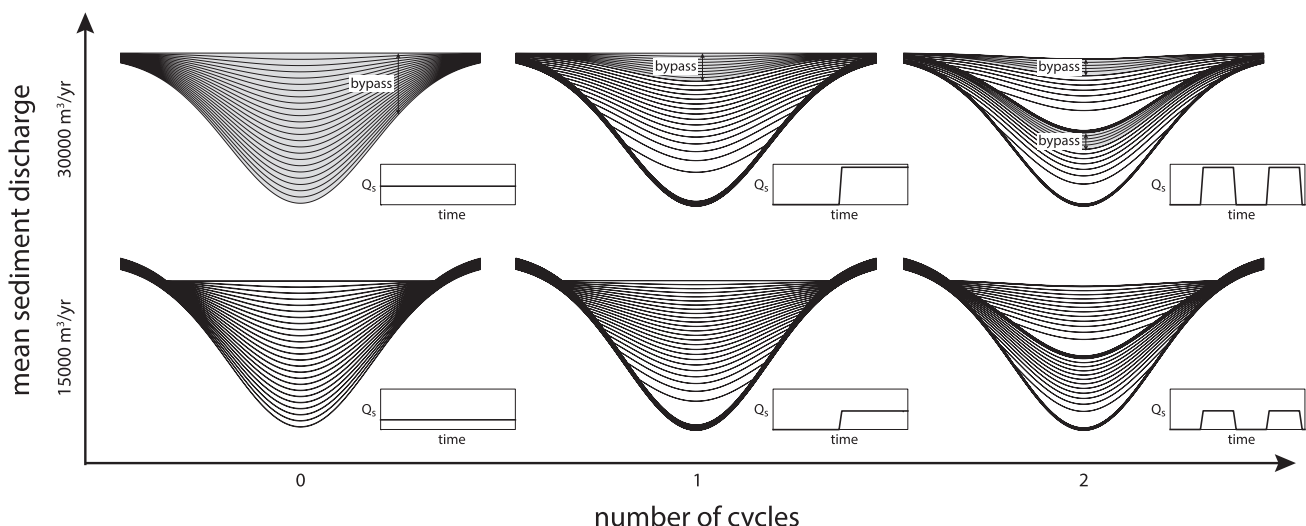


**Figure 19.** Summary of basin fill patterns as a function of number of sediment input cycles and mean sediment discharge. Insets show the sediment discharge curve for each case.

seismic facies (Prather et al., 1998; Booth et al., 2003), more sheet-like deposits are likely to converge toward the same pinchout line along the basin margin and thus form convergent seismic units. Overall, bypass intervals are likely to be less sand rich than ponded units, as sands are commonly bypassed to the next basin through channel systems, and only fine-grained overbank deposits are retained in the basin affected by bypass.

To improve our predictions of sand distribution in such settings, further work could include the use of optimization algorithms to constrain the sediment input curve and thus distinguish sand-rich intervals with high sedimentation rates from stratigraphic units with limited sand.

## CONCLUSIONS

We have investigated the formation of stratigraphic sequences in intraslope minibasins and the resulting large-scale stratigraphic patterns using a simple surface-based model. Our model focuses on the interplay between sediment input and subsidence; it assumes quasihorizontal initial depositional surfaces, includes sediment bypass when more sediment is available compared to basin volume, and assumes no erosion. The key findings can be summarized as follows:

1. Whether stratal termination points in a minibasin are moving toward the basin margin (onlap), basin center (offlap), or are stationary (convergence) is determined by the balance between the volume needed to accommodate the incoming sediment and the space made available through subsidence on top of the previous deposit (Figure 2).
2. When accommodation over the top of the previous deposit and sediment input equal each other over several time steps, perfect convergence develops (Figure 3). However, this configuration is unstable as any divergence from the balance between incoming sediment volume and space made available through subsidence will result in either onlap or offlap.
3. Cycles of increasing-to-decreasing sediment supply coupled with constant subsidence result in stratigraphic sequences with an onlapping lower part and offlapping upper part. Each sequence corresponds to one cycle of sediment input. The onlapping deposits are thicker, have higher-angle stratal terminations, and therefore are easier to identify than the offlapping units. Condensed sections separating the sequences overlie the offlap surface and underlie the onlap surface (Figure 5).
4. If the sediment input curve is more similar to a step function, with periods of no input alternating with high sediment supply, stratigraphic sequences only consist of an onlapping sediment package, with no offlap at the top (Figure 9). Large-scale stratigraphic patterns in Basin 4 of the Brazos-Trinity system can be well reproduced with a step-function model (Figure 14).
5. As subsidence commonly varies more slowly than sediment input, minibasins can fill relatively quickly and then oscillate between phases of bypass, when part of the sediment is transported downslope into the next basin, and phases of ponding, when all sediment is captured in the basin. Sequences with phases of bypass consist of three systems tracts: (1) onlapping unit at the base; (2) bypass deposits in the middle, characterized by stratal convergence in the model; and (3) offlapping unit at the top (Figure 6). If the sediment supply has an on-off nature, the sequences become more asymmetric and they only consist of the onlapping and bypass units.
6. Subsidence that varies through time (e.g., because of tectonic events) coupled with constant sediment input results in nonintuitive stratigraphic patterns: the sequence boundaries (onlap and offlap surfaces) are restricted to the basin margins and they correlate to deposits with the highest sedimentation rates in the basin center (Figure 7). However, if the sediment input varies through time as well, the influence of subsidence variability becomes difficult to recognize from the stratal patterns alone.
7. Static fill-and-spill models that do not include the influence of subsidence on sedimentation cannot provide an accurate representation of how sediment is distributed across intraslope basins. Models of dynamic fill-and-spill that capture the effect of ongoing subsidence during sedimentation suggest that basin fills can be largely coeval, if the long-term averages of volumetric sediment input and subsidence rates are of similar magnitudes (Figure 11).
8. Convergent baselapping stratal patterns form when sediment input rates are high compared to the subsidence rate and the existing

accommodation is significant. Convergent thinning is generated when (1) sediment input rates are lower, more similar to the volumetric subsidence rate calculated over the previous deposit, or (2) at times of sediment bypass. The higher rates of sediment input and accumulation during the formation of baselapping patterns are probably the reason why this facies tends to be more sand rich than the convergent thinning geometries.

9. Key aspects of the stratigraphic patterns in intra-slope basins can be summarized as a matrix of cross sections, with the number of sediment input cycles on the *x* axis and mean sediment discharge on the *y* axis (Figure 19). Onlap surfaces form as a result of episodic sediment input; increasing the average sediment discharge results in more pronounced bypass.

## REFERENCES CITED

- Allen, P. A., and J. R. Allen, 2005, Basin analysis: Principles and applications: Oxford, Blackwell Publishing, 549 p.
- Badalini, G., B. C. Kneller, and C. D. Winker, 2000, Architecture and processes in the late Pleistocene Brazos-Trinity turbidite system, Gulf of Mexico continental slope: Gulf Coast Section-SEPM Foundation 20th Annual Research Conference, Houston, Texas, December 3–6, 2000, p. 16–34.
- Bakke, K., I. A. Kane, O. J. Martinsen, S. A. Petersen, T. A. Johansen, S. Hustoft, F. Hadler-Jacobsen, and A. Groth, 2013, Seismic modeling in the analysis of deep-water sandstone termination styles: AAPG Bulletin, v. 97, no. 9, p. 1395–1419, doi:[10.1306/03041312069](https://doi.org/10.1306/03041312069).
- Beaubouef, R. T., and V. Abreu, 2006, Basin 4 of the Brazos-Trinity slope system: Anatomy of the terminal portion of an intra-slope lowstand systems tract: Gulf Coast Association of Geological Societies Transactions, v. 56, p. 39–49.
- Beaubouef, R. T., and S. J. Friedmann, 2000, High resolution seismic/sequence stratigraphic framework for the evolution of Pleistocene intra slope basins, Western Gulf of Mexico: Depositional models and reservoir analogs: Gulf Coast Section-SEPM Foundation 20th Annual Research Conference, Houston, Texas, December 3–6, 2000, p. 40–60.
- Booth, J. R., M. C. Dean, A. E. DuVernay III, and M. J. Styzen, 2003, Paleo-bathymetric controls on the stratigraphic architecture and reservoir development of confined fans in the Auger Basin: Central Gulf of Mexico slope: Marine and Petroleum Geology, v. 20, no. 6, p. 563–586, doi:[10.1016/j.marpetgeo.2003.03.008](https://doi.org/10.1016/j.marpetgeo.2003.03.008).
- Booth, J. R., A. E. DuVernay III, and D. S. Pfeiffer, 2000, Sequence stratigraphic framework, depositional models, and stacking patterns of ponded and slope fan systems in the Auger Basin: Central Gulf of Mexico slope: Gulf Coast Section-SEPM Foundation 20th Annual Research Conference, Houston, Texas, December 3–6, 2000, p. 82–103.
- Brunt, R., W. D. McCaffrey, and B. C. Kneller, 2004, Experimental modeling of the spatial distribution of grain size in a fill-and-spill mini-basin setting: Journal of Sedimentary Petrology, v. 74, no. 3, p. 438–446, doi:[10.1306/093003740438](https://doi.org/10.1306/093003740438).
- Christie-Blick, N., 1991, Onlap, offlap, and the origin of unconformity-bounded depositional sequences: Marine Geology, v. 97, no. 1–2, p. 35–56, doi:[10.1016/0025-3227\(91\)90018-Y](https://doi.org/10.1016/0025-3227(91)90018-Y).
- Covault, J. A., and B. W. Romans, 2009, Growth patterns of deep-sea fans revisited: Turbidite-system morphology in confined basins, examples from the California Borderland: Marine Geology, v. 265, no. 1–2, p. 51–66, doi:[10.1016/j.margeo.2009.06.016](https://doi.org/10.1016/j.margeo.2009.06.016).
- Giles, K. A., and T. F. Lawton, 2002, Halokinetic sequence stratigraphy adjacent to the El Papalote diapir, northeastern Mexico: AAPG Bulletin, v. 86, no. 5, p. 823–840.
- Giles, K. A., and M. G. Rowan, 2012, Concepts in halokinetic-sequence deformation and stratigraphy, in G. I. Alsop, S. G. Archer, A. J. Hartley, N. T. Grant, and R. Hodgkinson, eds., Salt tectonics, sediments and prospectivity: Geological Society, London, Special Publications, v. 363, p. 7–31, doi:[10.1144/SP363.2](https://doi.org/10.1144/SP363.2).
- Gorsline, D., and K. Emery, 1959, Turbidity-current deposits in San Pedro and Santa Monica basins off southern California: Geological Society of America Bulletin, v. 70, no. 3, p. 279–290, doi:[10.1130/0016-7606\(1959\)70\[279:TDISPA\]2.0.CO;2](https://doi.org/10.1130/0016-7606(1959)70[279:TDISPA]2.0.CO;2).
- Helland-Hansen, W., and G. J. Hampson, 2009, Trajectory analysis: Concepts and applications: Basin Research, v. 21, no. 5, p. 454–483, doi:[10.1111/j.1365-2117.2009.00425.x](https://doi.org/10.1111/j.1365-2117.2009.00425.x).
- Hudec, M., and M. P. A. Jackson, 2007, Terra infirma: Understanding salt tectonics: Earth Science Reviews, v. 82, no. 1–2, p. 1–28, doi:[10.1016/j.earscirev.2007.01.001](https://doi.org/10.1016/j.earscirev.2007.01.001).
- Hudec, M., M. P. A. Jackson, and D. D. Schultz-Ela, 2008, The paradox of minibasins subsidence into salt: Clues to evolution of crustal basins: Geological Society of America Bulletin, v. 121, no. 1/2, p. 201–221, doi:[10.1130/B26275.1](https://doi.org/10.1130/B26275.1).
- Jervey, M. T., 1988, Quantitative geological modeling of siliciclastic rock sequences and their seismic expression, in C. K. Wilgus, B. S. Hastings, H. Posamentier, J. Van Wagoner, C. A. Ross, and C. G. S. Kendall, eds., Sea-level changes: SEPM Special Publication, v. 42, p. 47–69.
- Kendrick, J. W., 2000, Turbidite reservoir architecture in the Northern Gulf of Mexico deepwater: Insights from the development of Auger, Tahoe, and Ram/Powell Fields: Gulf Coast Section-SEPM Foundation 20th Annual Research Conference, Houston, Texas, December 3–6, 2000, p. 450–468.
- Khan, S., and J. Imran, 2008, Numerical investigation of turbidity currents flowing through minibasins on the continental slope: Journal of Sedimentary Petrology, v. 78, no. 4, p. 245–257, doi:[10.2110/jsr.2008.031](https://doi.org/10.2110/jsr.2008.031).
- Lamb, M. P., T. Hickson, J. G. Marr, B. Sheets, C. Paola, and G. Parker, 2004, Surging versus continuous turbidity currents: Flow dynamics and deposits in an experimental

- intraslope basin: *Journal of Sedimentary Petrology*, v. 74, no. 1, p. 148–155, doi:[10.1306/062103740148](https://doi.org/10.1306/062103740148).
- Lamb, M. P., H. Toniolo, and G. Parker, 2006, Trapping of continuous turbidity currents by intraslope minibasins: *Sedimentology*, v. 53, no. 1, p. 147–160, doi:[10.1111/sed.2006.53.issue-1](https://doi.org/10.1111/sed.2006.53.issue-1).
- Lyons, W. J., 2004, Quantifying channelized submarine depositional systems from bed to basin scale: Ph.D. thesis, Massachusetts Institute of Technology, Cambridge, Massachusetts, 252 p.
- Madof, A. S., N. Christie-Blick, and M. H. Anders, 2009, Stratigraphic controls on a salt-withdrawal intraslope minibasin, north-central Green Canyon, Gulf of Mexico: Implications for misinterpreting sea level change: *AAPG Bulletin*, v. 93, no. 4, p. 535–561, doi:[10.1306/1222080802](https://doi.org/10.1306/1222080802).
- Mahaffie, M. J., 1994, Reservoir classification for turbidite intervals at the Mars discovery, Mississippi Canyon 807, Gulf of Mexico: Submarine fans and turbidite systems: *Gulf Coast Section-SEPM Foundation 15th Annual Research Conference*, December 4–7, 1994, p. 233–244.
- Mallarino, G., R. T. Beaubouef, A. W. Droxler, V. Abreu, and L. Labeyrie, 2006, Sea level influence on the nature and timing of a minibasin sedimentary fill (northwestern slope of the Gulf of Mexico): *AAPG Bulletin*, v. 90, no. 7, p. 1089–1119, doi:[10.1306/02210605058](https://doi.org/10.1306/02210605058).
- Meckel III, L. D., G. A. Ugueto, D. H. Lynch, and B. M. Hewett, 2002, Genetic stratigraphy, stratigraphic architecture, and reservoir stacking patterns of the upper Miocene–lower Pliocene greater Mars-Ursa intraslope basin, Mississippi Canyon, Gulf of Mexico: *Gulf Coast Section-SEPM Foundation 22nd Annual Research Conference*, Houston, Texas, December 8–11, 2002, p. 113–147.
- Muto, T., and R. J. Steel, 2000, The accommodation concept in sequence stratigraphy: Some dimensional problems and possible redefinition: *Sedimentary Geology*, v. 130, no. 1–2, p. 1–10, doi:[10.1016/S0037-0738\(99\)00107-4](https://doi.org/10.1016/S0037-0738(99)00107-4).
- Paola, C., 2000, Quantitative models of sedimentary basin filling: *Sedimentology*, v. 47, p. 121–178, doi:[10.1046/j.1365-3091.2000.00006.x](https://doi.org/10.1046/j.1365-3091.2000.00006.x).
- Paola, C., and J. M. Martin, 2012, Mass-balance effects in depositional systems: *Journal of Sedimentary Petrology*, v. 82, no. 6, p. 435–450, doi:[10.2110/jsr.2012.38](https://doi.org/10.2110/jsr.2012.38).
- Peel, F. J., 2014, How do salt withdrawal minibasins form? Insights from forward modeling, and implications for hydrocarbon migration: *Tectonophysics*, v. 630, p. 222–235, doi:[10.1016/j.tecto.2014.05.027](https://doi.org/10.1016/j.tecto.2014.05.027).
- Pérez, F., and B. E. Granger, 2007, IPython: A system for interactive scientific computing: *Computing in Science and Engineering*, v. 9, no. 3, p. 21–29, doi:[10.1109/MCSE.2007.53](https://doi.org/10.1109/MCSE.2007.53).
- Pilcher, R. S., B. Kilsdonk, and J. Trudeau, 2011, Primary basins and their boundaries in the deep-water northern Gulf of Mexico: Origin, trap types, and petroleum system implications: *AAPG Bulletin*, v. 95, no. 2, p. 219–240, doi:[10.1306/06301010004](https://doi.org/10.1306/06301010004).
- Pirmez, C., B. E. Prather, G. Mallarino, W. W. O'Hayer, A. W. Droxler, and C. D. Winker, 2012, Chronostratigraphy of the Brazos-Trinity depositional system, Western Gulf of Mexico: Implications for deepwater depositional models: *SEPM Special Publication*, v. 99, p. 111–143, doi:[10.2110/pec.12.99.0111](https://doi.org/10.2110/pec.12.99.0111).
- Posamentier, H. W., M. T. Jersey, and P. R. Vail, 1988, Eustatic controls on clastic deposition I—Conceptual framework: *SEPM Special Publication*, v. 42, p. 109–124.
- Prather, B. E., J. R. Booth, G. S. Steffens, and P. A. Craig, 1998, Classification, lithologic calibration, and stratigraphic succession of seismic facies of intraslope basins, deep-water Gulf of Mexico: *AAPG Bulletin*, v. 82, p. 701–728.
- Prather, B. E., C. Pirmez, Z. Sylvester, and D. S. Prather, 2012a, Stratigraphic response to evolving geomorphology in a submarine apron perched on the upper Niger Delta slope: *SEPM Special Publication*, v. 99, p. 145–161, doi:[10.2110/pec.12.99.0145](https://doi.org/10.2110/pec.12.99.0145).
- Prather, B. E., C. Pirmez, and C. D. Winker, 2012b, Stratigraphy of linked intraslope basins: Brazos-Trinity system, Western Gulf of Mexico: *SEPM Special Publication*, v. 99, p. 83–109, doi:[10.2110/pec.12.99.0083](https://doi.org/10.2110/pec.12.99.0083).
- Pratson, L. F., and W. B. F. Ryan, 1994, Pliocene to recent infilling and subsidence of intraslope basins offshore Louisiana: *AAPG Bulletin*, v. 78, no. 10, p. 1483–1506.
- Pyrcz, M. J., O. Catunenau, and C. V. Deutsch, 2005, Stochastic surface-based modeling of turbidite lobes: *AAPG Bulletin*, v. 89, no. 2, p. 177–191, doi:[10.1306/09220403112](https://doi.org/10.1306/09220403112).
- Reilly, M. J., and P. B. Flemings, 2010, Deep pore pressures and seafloor venting in the Auger Basin, Gulf of Mexico: *Basin Research*, v. 22, no. 4, p. 380–397, doi:[10.1111/j.1365-2117.2010.00481.x](https://doi.org/10.1111/j.1365-2117.2010.00481.x).
- Rowan, M. G., T. F. Lawton, K. A. Giles, and R. A. Ratliff, 2003, Near-salt deformation in La Popa basin, Mexico, and the northern Gulf of Mexico: A general model for passive diapirism: *AAPG Bulletin*, v. 87, no. 5, p. 733–756, doi:[10.1306/01150302012](https://doi.org/10.1306/01150302012).
- Ryan, W. B. F., et al., 2009, Global multi-resolution topography synthesis: *Geochemistry, Geophysics, Geosystems*, v. 10, no. 3, p. 1–9, doi:[10.1029/2008GC002332](https://doi.org/10.1029/2008GC002332).
- Satterfield, W. M., and E. W. Behrens, 1990, A late Quaternary canyon/channel system, northwest Gulf of Mexico continental slope: *Marine Geology*, v. 92, no. 1–2, p. 51–67, doi:[10.1016/0025-3227\(90\)90026-G](https://doi.org/10.1016/0025-3227(90)90026-G).
- Schultz-Ela, D. D., 2003, Origin of drag folds bordering salt diapirs: *AAPG Bulletin*, v. 87, no. 5, p. 757–780, doi:[10.1306/12200201093](https://doi.org/10.1306/12200201093).
- Sinclair, H., and M. Tomasso, 2002, Depositional evolution of confined turbidite basins: *Journal of Sedimentary Petrology*, v. 72, no. 4, p. 451–456, doi:[10.1306/111501720451](https://doi.org/10.1306/111501720451).
- Smith, R. D., 2004, Silled sub-basins to connected tortuous corridors: Sediment distribution systems on topographically complex sub-aqueous slopes: *Geological Society, London, Special Publications*, v. 222, no. 1, p. 23–43, doi:[10.1144/GSL.SP.2004.222.01.03](https://doi.org/10.1144/GSL.SP.2004.222.01.03).
- Smith, R. D., and P. Joseph, 2004, Onlap stratal architectures in the Gres d'Annot: Geometric models and controlling factors, in P. Joseph and S. A. Lomas, eds., *Deep-water sedimentation in the Alpine basin of SE France*: New

- perspectives on the Grès d'Annot and related systems: Geological Society, London, Special Publications, v. 221, no. 1, p. 389–399, doi:[10.1144/GSL.SP.2004.221.01.21](https://doi.org/10.1144/GSL.SP.2004.221.01.21).
- Steffens, G. S., E. K. Biegert, H. S. Sumner, and D. Bird, 2003, Quantitative bathymetric analyses of selected deep-water siliciclastic margins: Receiving basin configurations for deepwater fan systems: *Marine and Petroleum Geology*, v. 20, no. 6, p. 547–561, doi:[10.1016/j.marpetgeo.2003.03.007](https://doi.org/10.1016/j.marpetgeo.2003.03.007).
- Straub, K. M., C. Paola, D. Mohrig, M. A. Wolinsky, and T. George, 2009, Compensational stacking of channelized sedimentary deposits: *Journal of Sedimentary Petrology*, v. 79, no. 9, p. 673–688, doi:[10.2110/jsr.2009.070](https://doi.org/10.2110/jsr.2009.070).
- Teng, L. S., and D. S. Gorsline, 2008, Stratigraphic framework of the continental borderland basins, southern California, in J. P. Dauphin and B. R. T. Simonett, eds., *The Gulf and Peninsular Province of the Californias: AAPG Memoir 47*, p. 127–143.
- Toniolo, H., M. P. Lamb, and G. Parker, 2006a, Depositional turbidity currents in diapiric minibasins on the continental slope: Formulation and theory: *Journal of Sedimentary Petrology*, v. 76, no. 5, p. 783–797, doi:[10.2110/jsr.2006.071](https://doi.org/10.2110/jsr.2006.071).
- Toniolo, H., G. Parker, V. Voller, and R. T. Beaubouef, 2006b, Depositional turbidity currents in diapiric minibasins on the continental slope: Experiments-numerical simulation and upscaling: *Journal of Sedimentary Petrology*, v. 76, no. 5, p. 798–818, doi:[10.2110/jsr.2006.072](https://doi.org/10.2110/jsr.2006.072).
- Vail, P. R., R. M. Mitchum, and J. S. Thompson III, 1977, Seismic stratigraphy and global changes of sea level, Part 3: Relative changes of sea level from coastal onlap, in C. E. Payton, ed., *Seismic stratigraphy: Applications to Hydrocarbon Exploration: AAPG Memoir 26*, p. 63–81.
- Viparelli, E., T. Yeh, A. Cantelli, E. Leslie, A. Robertson, and G. Parker, 2012, Stratigraphy of linked submarine minibasins in laboratory experiments: AAPG Search and Discovery Article #40960, accessed February 11, 2015, [http://www.searchanddiscovery.com/pdfz/documents/2012/40960viparelli/ndx\\_viparelli.pdf.html](http://www.searchanddiscovery.com/pdfz/documents/2012/40960viparelli/ndx_viparelli.pdf.html).
- Winker, C. D., 1996, High-resolution seismic stratigraphy of a late Pleistocene submarine fan ponded by salt-withdrawal mini-basins on the Gulf of Mexico continental slope: Proceedings of the 28th Annual Offshore Technology Conference, Houston, Texas, May 6–9, 1996, p. 619–628, doi:[10.4043/8024-MS](https://doi.org/10.4043/8024-MS).
- Winker, C. D., and J. R. Booth, 2000, Sedimentary dynamics of the salt-dominated continental slope, Gulf of Mexico: Integration of observations from the seafloor, near-surface, and deep subsurface: Gulf Coast Section-SEPM Foundation 20th Annual Research Conference, Houston, Texas, December 3–6, 2000, p. 1059–1086.